

**AD-A279 440**



**N74-23394**  
**PERSONAL COPY**

**NASA TECHNICAL  
MEMORANDUM**

**NASA TM X-71956**  
**COPY NO.**

6

**NASA TM X-71956**

**SUPERSONIC AND HYPERSONIC AERODYNAMIC  
CHARACTERISTICS OF TWO SHUTTLE-ORBITER  
CONFIGURATIONS DESIGNED FOR REDUCED LENGTH**

**Howard W. Stone**

**DTIC**  
**S ELECTE D**  
**MAY 16 1994**  
**F**

**April 1974**

**94-14495**



**This document has been approved  
for public release and sale; its  
distribution is unlimited.**

**This informal documentation medium is used to provide accelerated or  
special release of technical information to selected users. The contents  
may not meet NASA formal editing and publication standards, may be re-  
vised, or may be incorporated in another publication.**

**NATIONAL AERONAUTICS AND SPACE ADMINISTRATION  
LANGLEY RESEARCH CENTER, HAMPTON, VIRGINIA 23665**

**94 5 13 127**

**DTIC QUALITY ASSURANCE**

1. Report No. NASA TM X-71956		2. Government Accession No.		3. Recipient's Catalog No.	
4. Title and Subtitle Supersonic and Hypersonic Aerodynamic Characteristics of Two Shuttle-Orbiter Configurations Designed for Reduced Length				5. Report Date April 1974	
				6. Performing Organization Code	
7. Author(s) Howard W. Stone				8. Performing Organization Report No.	
9. Performing Organization Name and Address NASA Langley Research Center Hampton, VA 23665				10. Work Unit No.	
				11. Contract or Grant No.	
12. Sponsoring Agency Name and Address NASA				13. Type of Report and Period Covered Technical Memorandum	
				14. Sponsoring Agency Code	
15. Supplementary Notes Special technical information release, not planned for formal NASA publication.					
16. Abstract  Performance, stability, and control tests at supersonic and hypersonic speeds have been performed on two versions of a shuttle orbiter configuration designed for reduced length. One of the test configurations had twin dorsal fins rolled out $15^\circ$ , the other a centerline single dorsal fin. Effects of elevon and body flap deflection, rudder flare, planform fillet, and aileron deflection were examined. The supersonic tests were over the Mach number range from 1.6 to 4.63 at a Reynolds number based on model length of $4.3 \times 10^6$ . The hypersonic tests were conducted at a Mach number of 10.3 and Reynolds number of $0.67 \times 10^6$ .					
17. Key Words (Suggested by Author(s)) (STAR category underlined) <u>Aerodynamics</u> Supersonic and hypersonic <u>Space Vehicles</u>				18. Distribution Statement  Unclassified - Unlimited	
19. Security Classif. (of this report) Unclassified		20. Security Classif. (of this page) Unclassified		21. No. of Pages 52	
				22. Price* \$3.75	

\* Available from { The National Technical Information Service, Springfield, Virginia 22151  
STIF/NASA Scientific and Technical Information Facility, P.O. Box 33, College Park, MD 20740

# SUPERSONIC AND HYPERSONIC AERODYNAMIC CHARACTERISTICS OF TWO SHUTTLE-ORBITER CONFIGURATIONS DESIGNED FOR REDUCED LENGTH

Howard W. Stone

## SUMMARY

Performance, stability, and control tests at supersonic and hypersonic speeds have been performed on two versions of a shuttle orbiter configuration designed for reduced length. One of the test configurations had twin dorsal fins rolled out  $15^\circ$  and the other, a centerline single dorsal fin. Effects of elevon and body flap deflection, rudder flare, planform fillet, and aileron deflection were examined. The supersonic tests were conducted over the Mach number range from 1.6 to 4.63 at a Reynolds number based on model length of  $4.3 \times 10^6$ . The hypersonic tests were conducted at a Mach number of 10.3 and Reynolds number of  $0.67 \times 10^6$ .

The  $M=10.3$  results show that the twin fin version has stable trim capability at  $30^\circ$  angle of attack for centers of gravity between 63.3 percent and 66.6 percent of fuselage reference length for a range of elevon and body flap deflection angles of  $-40^\circ$  to  $0^\circ$  and  $-25^\circ$  to  $0^\circ$ . This configuration is slightly unstable directionally with positive effective dihedral at this Mach number. The yaw due to roll control is adverse for an elevon deflection of  $-10^\circ$  and favorable for an elevon deflection of  $-30^\circ$ . The former results in a roll reversal motion due to aileron control and a near zero value of the roll effectiveness parameter at the latter indicates insufficient control authority to maintain a vehicle rolling motion.

With  $\pm 30^\circ$  of rudder flare, the single fin version is statically stable in pitch and requires down elevon deflection to trim over much of the angle-of-attack range at the low supersonic Mach numbers for all center-of-gravity positions of interest. The  $60^\circ$  swept planform wing fillet, however, had small effect on the longitudinal characteristics at the higher supersonic Mach numbers. At a Mach number of 10.3, the single fin version has stable trim capability at  $30^\circ$  angle of attack for centers of gravity between 63.4 percent and 70.4 percent of the fuselage reference length with the planform fillet off and between 63.1 percent and 70.0 percent with the fillet on over a range of elevon and body flap deflection angles of  $-40^\circ$  to  $+10^\circ$  and  $-25^\circ$  to  $+10^\circ$ , respectively. The planform fillet also resulted in a slightly higher lift coefficient at the higher angles of attack.

Availability Codes	
Dist	Avail and/or Special
A-1	

Supersonically, the single fin version was directionally stable below about  $18^\circ$  angle of attack for a  $30^\circ$  flared rudder and directionally unstable hypersonically at all angles of attack with an unflared rudder. The configuration had positive effective dihedral at nearly all positive angles of attack supersonically with the fin on and hypersonically with and without the center dorsal fin.

## INTRODUCTION

During the past few years, the NASA, USAF, and the aerospace industry have investigated several approaches to providing a cost effective system capable of transferring large payloads to and from near-earth orbit. The history and mission profile of the system now under development are presented in reference 1. The orbiter configuration in this system has large doors on the top of the vehicle for payload bay access. An alternate orbiter concept examined at the Langley Research Center had the payload bay access at the aft end of the fuselage with the rocket engines located alongside the payload bay. Such a design approach makes it possible to reduce the vehicle length and weight and increase structural stiffness.

This paper presents experimental performance, stability, and control data on alternate configurations designed for reduced length. One configuration has twin dorsal fins located over the rocket motors installed on either side of the payload. This configuration minimizes the base area in that the base area is little more than the cross-sectional area of the payload bay plus two rocket engines. Experimental subsonic aerodynamic characteristics of this configuration are presented in reference 2. The second configuration has a single dorsal fin and a smooth fairing between the payload bay and the rocket motors. This fairing increases the base area and the internal volume while decreasing the wetted area. The increased volume can be used efficiently to carry several thousand pounds of propellant internally. Hypersonic wind-tunnel data are presented herein for the twin dorsal fin configuration and supersonic and hypersonic data are presented for the single dorsal fin configuration.

## SYMBOLS

The lateral-directional data are referred to the body-axis systems. Values are given in both SI and U.S. customary units.

b	wing span
$\bar{c}$	wing mean aerodynamic chord
$C_A$	axial force coefficient, $\frac{\text{Axial force}}{q_\infty S}$
$C_D$	drag coefficient, $\frac{\text{Drag}}{q_\infty S}$
$C_L$	lift coefficient, $\frac{\text{Lift}}{q_\infty S}$
$C_{\ell}$	rolling moment coefficient, $\frac{\text{Rolling moment}}{q_\infty S b}$

$$C_{l\beta} = \frac{\Delta C_l}{\Delta \beta}, \text{ per degree}$$

$$C_{l\delta_a} = \frac{\Delta C_l}{\delta_a}, \text{ per degree}$$

$$C_m \quad \text{pitching moment coefficient, } \frac{\text{Pitching moment}}{q_\infty S c}$$

$$C_N \quad \text{normal force coefficient, } \frac{\text{Normal force}}{q_\infty S}$$

$$C_n \quad \text{yawing-moment coefficient, } \frac{\text{Yawing moment}}{q_\infty S b}$$

$$C_{n\beta} = \frac{\Delta C_n}{\Delta \beta}, \text{ per degree}$$

$$C_{n\delta_a} = \frac{\Delta C_n}{\delta_a}, \text{ per degree}$$

$$C_Y \quad \text{side force coefficient, } \frac{\text{Side force}}{q S}$$

$$C_{Y\beta} = \frac{\Delta C_Y}{\Delta \beta}, \text{ per degree}$$

L/D lift-drag ratio

$l$  fuselage reference length (nose to body-flap hingeline)

M free stream Mach number

$q_\infty$  free stream dynamic pressure

R Reynolds number based on fuselage reference length

S reference wing planform area

$\alpha$  angle of attack, deg.

$\beta$  angle of sideslip, deg.

$\delta_a$  aileron deflection,  $\frac{\delta_{e,L} - \delta_{e,R}}{2}$ , degree

$\delta_e$  elevon deflection,  $\frac{\delta_{e,L} + \delta_{e,R}}{2}$ , deg. (positive for trailing edge down)

$\delta_f$  body flap deflection (positive for trailing edge down), deg.  
 $\omega_\phi/\omega_d^2$  roll effectiveness parameter

Subscripts:

L left  
 R right

### Description of Models


The end-loaded orbiter configurations that were tested in this investigation are sketched in figures 1 and 2. The pertinent dimensions of the twin fin version, shown in figure 1, are presented in Table I. A 0.0075 scale model was tested at  $M = 10.3$  with the twin dorsal fins rolled out  $15^\circ$  but without simulated rocket nozzles. The estimated entry payload out center of gravity was located at  $.65\bar{\ell}$  from the nose which corresponds to  $0.28\bar{c}$ .

A 0.01875 scale model of the single fin version (figure 2) was tested at supersonic speeds and a 0.0075 scale model (simulated engine nozzles off) at Mach 10.3. The tests were conducted with and without a wing planform fillet and also with and without a centerline fin. The rudder was flared  $\pm 30^\circ$  for all fin-on tests at supersonic speeds. The estimated entry payload out center of gravity for this version was located at  $0.68\bar{\ell}$  aft of the nose which corresponds to  $0.18\bar{c}$ .

The center of gravity was estimated to be located at  $0.12\bar{\ell}$  below the fuselage upper surface.

### Test Apparatus and Conditions

The supersonic tests were conducted in both the low and high Mach number test sections of the Langley Unitary Plan wind tunnel - the hypersonic tests in the Continuous Flow Hypersonic Tunnel, reference 3. All test conditions are presented below:

<u>Mach Number</u>	<u>Temperature</u>	<u>Dynamic Pressure</u> <u>n/m<sup>2</sup> (psf)</u>	<u>Reynolds Number</u>
1.6	66°C (150°F)	28,800 (601)	$4.3 \times 10^6$  $0.67 \times 10^6$
1.9	66°C (150°F)	28,700 (600)	
2.36	66°C (150°F)	26,900 (461)	
2.86	66°C (150°F)	23,700 (495)	
3.96	79°C (175°F)	17,600 (368)	
4.63	79°C (175°F)	13,900 (291)	
10.3	760°C (1400°F)	7,230 (151)	

The force and moment data were measured by sting-mounted, internal, six-component, strain-gage balances attached through the model base. The supersonic tests utilized a straight sting while the hypersonic tests utilized a straight sting for low angles of attack ( $0$  to  $35^\circ$ ) and a bent sting from  $20^\circ$  to  $50^\circ$  angle of attack. The bent sting, located at the top of the base, extended approximately 0.023 meters (0.9 inches) beyond the trailing edge of the body flap and then bent upward at a  $30^\circ$  angle (see model photograph, figure 1b). All the bent sting tests were without the center dorsal fin.

Transition strips were applied to the model for the high supersonic Mach number tests of planform fillet effect. The strips, 0.002 meters (1/16-inch) wide, of 45 grit were located 0.03 meters (1.2 inches) behind the body nose and 0.01 meters (0.4 inches) behind the wing and vertical tail leading edges. In all cases, the coefficients presented herein represent the gross values since no correction for base drag was included.

## RESULTS AND DISCUSSION

### Twin Fin Version Characteristics

Longitudinal.- The effects of elevon and body flap deflection on the longitudinal stability and performance at Mach 10.3 are shown in figure 3. The configuration has rather typical delta-wing shuttle performance characteristics ( $L/D_{\max} \approx 2$  occurs between  $15^\circ$  and  $20^\circ$  angle of attack, maximum lift occurring at  $\alpha > 50^\circ$ ). The configuration trims stably from  $15^\circ$  to  $45^\circ$  angle of attack for the center of gravity at 0.65 $\bar{x}$  using elevon and body flap deflections. At  $30^\circ$  angle of attack, moment transfer calculations indicate that the configuration has stable trim points for center-of-gravity positions between 63.3 and 66.6 percent of the fuselage reference length. This center-of-gravity range could be increased by downward deflection of elevons and body flap.

The contribution of the body flap to the longitudinal characteristics for  $\delta_e = 0$  is shown in figure 4. Moment transfer calculations show that body flap deflections from  $0$  to  $-25^\circ$  account for 0.9 percent of the 3.3 percent center-of-gravity range at  $\alpha = 30^\circ$ . This flap has a full scale chord of 1.68 meters (5.5 feet) and span of 10.8 meters (35.5 feet) and serves as a heat shield for the rocket nozzles during entry as well as a trim device.

Lateral-Directional.- Although the twin dorsal fins without rudder flare provide a stabilizing increment to the directional stability as is shown in figure 5, the increment is insufficient to stabilize the vehicle about the 65 percent  $\bar{x}$  center of gravity. The lack of directional stability is typical of this type of configuration



at these angles of attack and hypersonic speeds. The forebody and the wing act as shields forcing a leeside low dynamic pressure flow generally complicated by the presence of vortices to impinge on the dorsal fins rendering them relatively ineffective. These fins have negligible contribution to the effective dihedral down to  $15^\circ$  angle of attack; note the wings have  $7^\circ$  of dihedral. The elevon and body flap effects on the lateral-directional stability with  $15^\circ$  rolled out fins are shown in figure 6.

Roll control data for two elevon deflection angles is shown in figure 7. The control has adverse yaw output for  $\delta_e = -10^\circ$  but has a favorable yaw output for  $\delta_e = -30^\circ$  even though the elevon hingeline is swept rearward. Calculation of the roll effectiveness parameter  $(\omega_\phi/\omega_d)^2$  (see reference 4), reveals that for  $\delta_e = -10^\circ$ , a roll reversal motion will result from an aileron input at all angles of attack, i.e.  $(\omega_\phi/\omega_d)^2 < 0$ . For  $\delta_e = -30^\circ$ , the roll effectiveness parameter is very near zero throughout the angles of attack range tested. A zero value of this parameter is indicative of the inability of the control to sustain a vehicle rolling motion. A coordinated turn requires a roll effectiveness parameter value near unity (see simulation results in reference 4). Therefore, the near zero value for  $\delta_e = -30^\circ$  will result in unsatisfactory pilot ratings for aileron alone control, doing little more than exciting the Dutch roll oscillation.

#### Single Fin Version Characteristics

Longitudinal.— Results of the supersonic tests of the single fin configuration are presented in figures 8 and 9 and the hypersonic tests in figures 10 and 11. The data for the lower supersonic Mach numbers (see figure 8) show that the addition of the dorsal fin with  $\pm 30^\circ$  rudder flare increases the stability level and the trim angle of attack and, thus, requires some down elevon deflection to trim at the lower angles of attack and more aft center-of-gravity locations. There is also a slight tendency to pitchup and a reduction in the lift curve slope at the higher angles of attack. At the higher supersonic Mach numbers, the addition of a  $60^\circ$  swept planform fillet had little effect on the aerodynamic characteristics (see figure 9). The fillet is approximately  $1/8$  of the exposed wing area and extends to just beyond  $1/2$  the exposed wing span. Down elevon deflection will be required to trim about the more aft centers of gravity below an angle of attack of about  $34^\circ$ .

The hypersonic longitudinal characteristics at the lower angles of attack with the planform fillet off are shown in figure 10. The large nose-up moment for  $\delta_e = -40^\circ$  at low angles of attack is due to flow impingement on the upper surface of the highly deflected elevon. In figure 11, the higher angle-of-attack bent-sting, hypersonic test results are presented for the configuration with and without the planform fillet. The fillet was ahead of the center of gravity and, therefore, resulted in

a positive pitching moment increment particularly at the higher angles of attack. Moment transfer calculations indicate that at  $30^\circ$  angle of attack, the configuration has stable trim points for centers of gravity between 63.4 percent and 70.4 percent of the fuselage reference length with the fillet off and 63.1 percent and 70.0 percent with the fillet on for the range of elevon and body flap deflection angles tested. The higher leading edge sweep angle of the fillet ( $60^\circ$  versus  $50^\circ$  for wing) reduced axial force. The added planform area increased normal force, and therefore lift, particularly at the higher angles of attack.

Lateral-Directional.- Fin-on and off data are presented in figure 12 for Mach numbers 1.6 to 2.86. At all Mach numbers, the fin-on configuration with a  $\pm 30^\circ$  rudder flare had positive effective dihedral over the test angle-of-attack range. The configuration is directionally stable below about  $18^\circ$  angle of attack with some tail effectiveness continuing until about  $24^\circ$  at these Mach numbers. The addition of the planform fillet (figure 13) had negligible effect on the lateral-directional stability characteristics and the configuration continued to exhibit directional stability below about  $18^\circ$  angle of attack at the higher supersonic Mach numbers. The configuration is directionally unstable hypersonically at all angles of attack (figure 14); however, the positive effective dihedral at nearly all attitudes results in a positive dynamic directional stability parameter above about  $15^\circ$  angle of attack for an estimated inertia ratio of 7. The fillet has a slight adverse effect on the directional stability.

## CONCLUSIONS

Supersonic and hypersonic characteristics of two versions of a shuttle orbiter configuration designed for reduced length have been determined through wind-tunnel tests. The results indicate that:

1. The twin fin configuration has stable trim capability at  $30^\circ$  angle of attack for centers of gravity between 63.3 percent and 66.6 percent of fuselage reference length for a range of elevon and body flap deflections of  $-40^\circ$  to  $0^\circ$  and  $-25^\circ$  to  $0^\circ$ , respectively, at a Mach number of 10.3.
2. The twin fin version with  $15^\circ$  rolled out dorsal fins is slightly unstable directionally at Mach 10.3; the effective dihedral is positive. The fins provide a stable increment in directional stability even at the higher angles of attack.
3. The twin fin version with a rearward swept elevon hingeline has adverse yaw due to roll control for an elevon deflection of  $-10^\circ$  and favorable yaw due to roll control for an elevon deflection of  $-30^\circ$ . The former results in a roll reversal motion due to aileron control and the latter a roll effectiveness parameter value near zero which indicates insufficient control authority to maintain a vehicle rolling motion.

4. With  $\pm 30^\circ$  of rudder flare, the single fin version has longitudinal static stability and requires down elevon deflection to trim over much of the angle-of-attack range at the low supersonic Mach numbers for all center-of-gravity positions of interest. The  $60^\circ$  swept planform wing fillet had a small effect on the longitudinal characteristics at the higher supersonic Mach numbers.

5. At a Mach number of 10.3, the single fin version has stable trim capability at  $30^\circ$  angle of attack for centers of gravity between 63.4 percent and 70.4 percent of the fuselage reference length with the planform fillet off and between 63.1 percent and 70.0 percent with the fillet on over a range of elevon and body flap deflection angles of  $-40^\circ$  to  $+10^\circ$  and  $-25^\circ$  to  $+10^\circ$ , respectively. The planform fillet also resulted in a slightly higher lift coefficient at the higher angles of attack.

6. Supersonically, the single fin version was directionally stable below about  $18^\circ$  angle of attack for a  $\pm 30^\circ$  flared rudder and directionally unstable hypersonically at all angles of attack with an unflared rudder. The configuration had positive effective dihedral at nearly all positive angles of attack supersonically with the fin on and hypersonically with and without the center dorsal fin.

#### REFERENCES

1. Love, Eugene S.: Advanced Technology and the Space Shuttle. Astronautics and Aeronautics, February 1973.
2. Ware, George M.; and Spencer, Bernard, Jr.: Low Subsonic Aerodynamic Characteristics of a Shuttle-Orbiter Configuration Designed for Reduced Length. NASA TM X-2712, April 1973.
3. Pirrello, C. J.; Hardin, R. D.; Heckert, M. V.; and Brown, K. R.: An Inventory of Aeronautical Ground Research Facilities. Vol. I - Wind Tunnels, NASA CR-1874, 1971.
4. Behm, William F.: An Aerodynamic Entry Control Technique Utilizing the Yaw Flap Concept. Presented at AIAA Guidance and Control Conference, August 20-22, 1973, Key Biscayne, Florida. Paper No. 73-888.

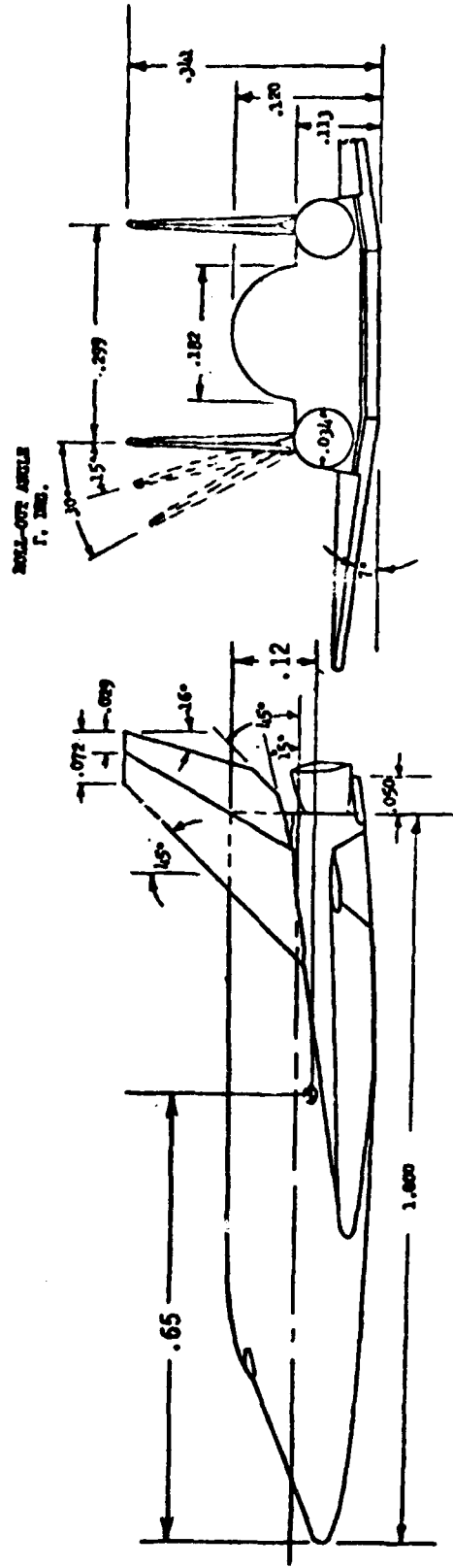
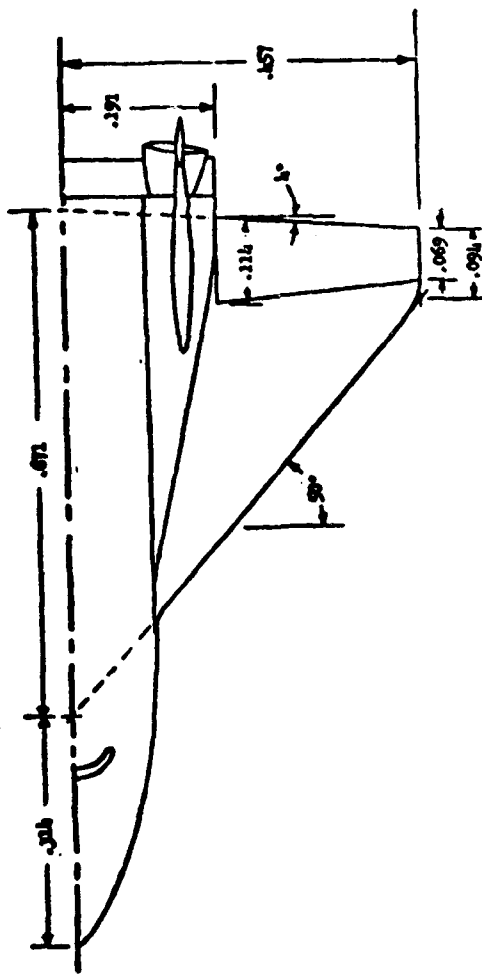
Table I

## CONFIGURATION CHARACTERISTICS (FULL-SIZE)

	<u>Twin Fin Version</u>	<u>Single Fin Version</u>
<u>Fuselage</u>		
Body length, m (ft)	28.3 (92.9)	28.3 (92.9)
Nose to body flap hingeline, m (ft) (fuselage reference length, $\ell$ )	28.1 (92.1)	28.1 (92.1)
Nose radius, m (ft)	0.38 (1.25)	0.66 (2.17)
Base area, $m^2$ ( $ft^2$ )	36.5 (393)	39.8 (428)
<u>Body Flap</u>		
Area, $m^2$ ( $ft^2$ )	18.1 (195)	18.1 (195)
Chord, m (ft)	1.68 (5.5)	1.68 (5.5)
Span, m (ft)	10.8 (35.5)	10.8 (35.5)
<u>Wing</u>		
Theoretical root chord at body center- line, m (ft)	18.6 (61.1)	18.6 (61.1)
Tip chord, m (ft)	2.67 (8.75)	2.67 (8.75)
Reference area, $S$ , $m^2/ft$	279 (3004)	279 (3004)
Mean aerodynamic chord, $\bar{c}$ , m (ft)	12.8 (41.9)	12.8 (41.9)
Span, $b$ , m (ft)	25.9 (85.0)	25.9 (85.0)
Aspect ratio	2.4	2.4
Taper ratio	.14	.14
Sweep: leading edge	$50^\circ$	$50^\circ$
trailing edge	$-4^\circ$	$-4^\circ$
Elevon area, $m^2$ ( $ft^2$ )	39.8 (428)	39.8 (428)
Dihedral	$7^\circ$	$7^\circ$
Incidence: at body	$2^\circ$	$2^\circ$
at top	$-3^\circ$	$-3^\circ$
Airfoil section: theoretical root body centerline)	NACA 0008-64	NACA 0008-64
Airfoil section: tip	NACA 0012-64	NACA 0012-64
Fillet: sweep	None	$60^\circ$
area, $m^2$ ( $ft^2$ )		16.7 (180)
Theoretical apex aft of nose, m/ft	8.90 (29.2)	11.0 (36.1)
<u>Vertical Tail</u>		
Root chord, m (ft)	7.32 (24.0)	7.32 (24.0)
Tip chord, m (ft)	3.38 (11.1)	3.38 (11.1)
Exposed area, $m^2$ ( $ft^2$ )	39.9 (430)	39.9 (430)

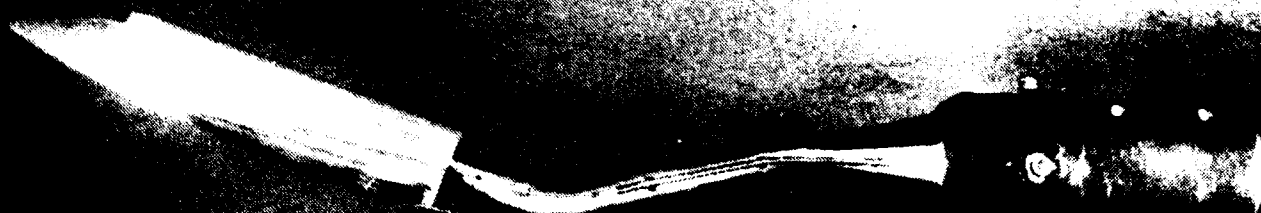
Table I - Continued:

Rudder area, m <sup>2</sup> (ft <sup>2</sup> )	16.0 (172)	16.0 (172)
Aspect ratio	1.39	1.39
Sweep: leading edge	45°	45°
trailing edge	25°	25°
Taper ratio	.46	.46
Airfoil section	NACA 0012-64	NACA 0012-64
<u>Center-of-Gravity Locations</u>		
Aft of nose: (% ref. length)	65%	68%
(% c)	27.7%	17.7%
Below fuselage upper surface	12%	12%



(a) Configuration sketch. All dimensions normalized to body reference length.

Figure 1 - Twin Fin Version.



(b) Hypersonic model installation photograph (dorsal fins off).

Figure 1. - Concluded.

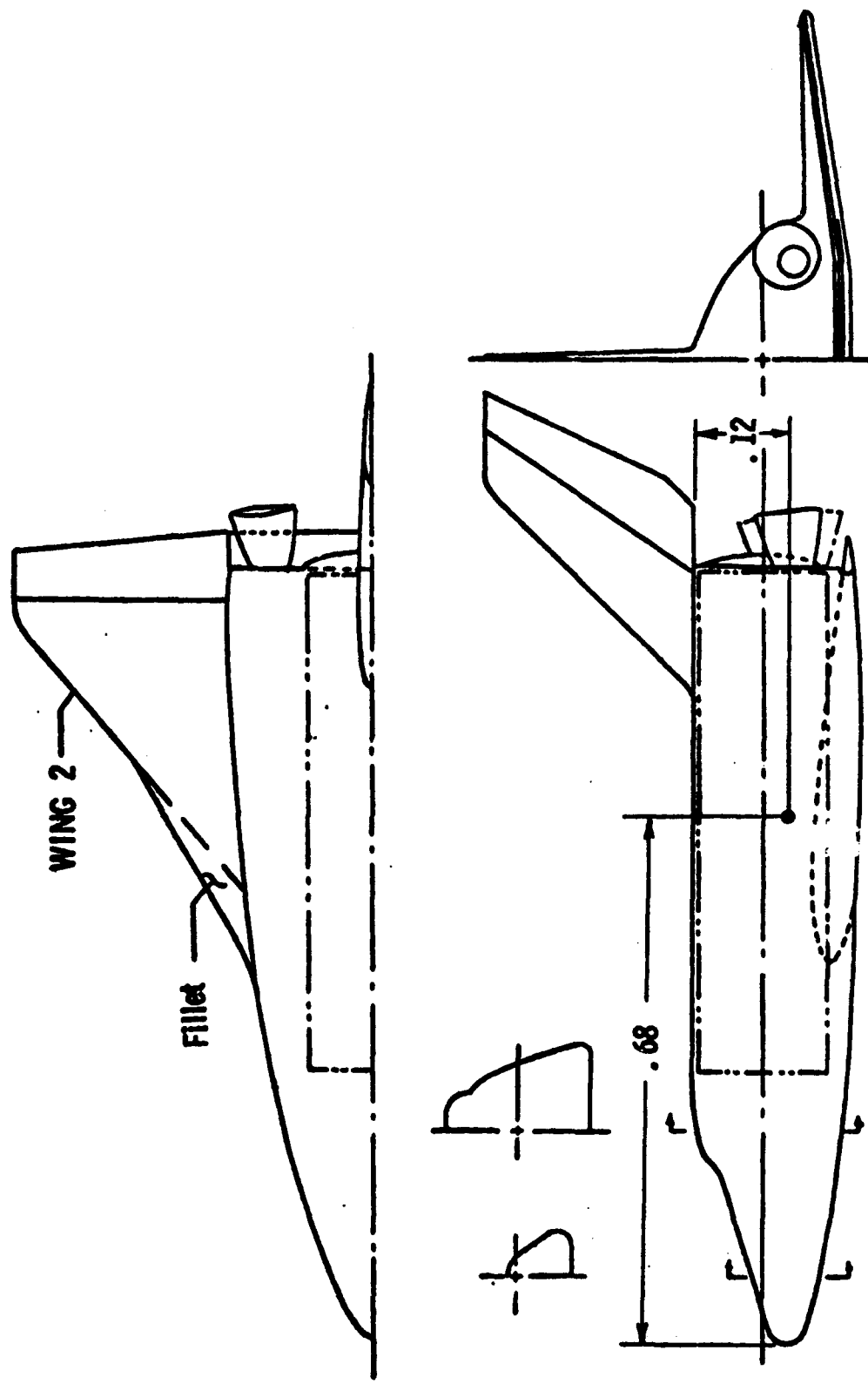
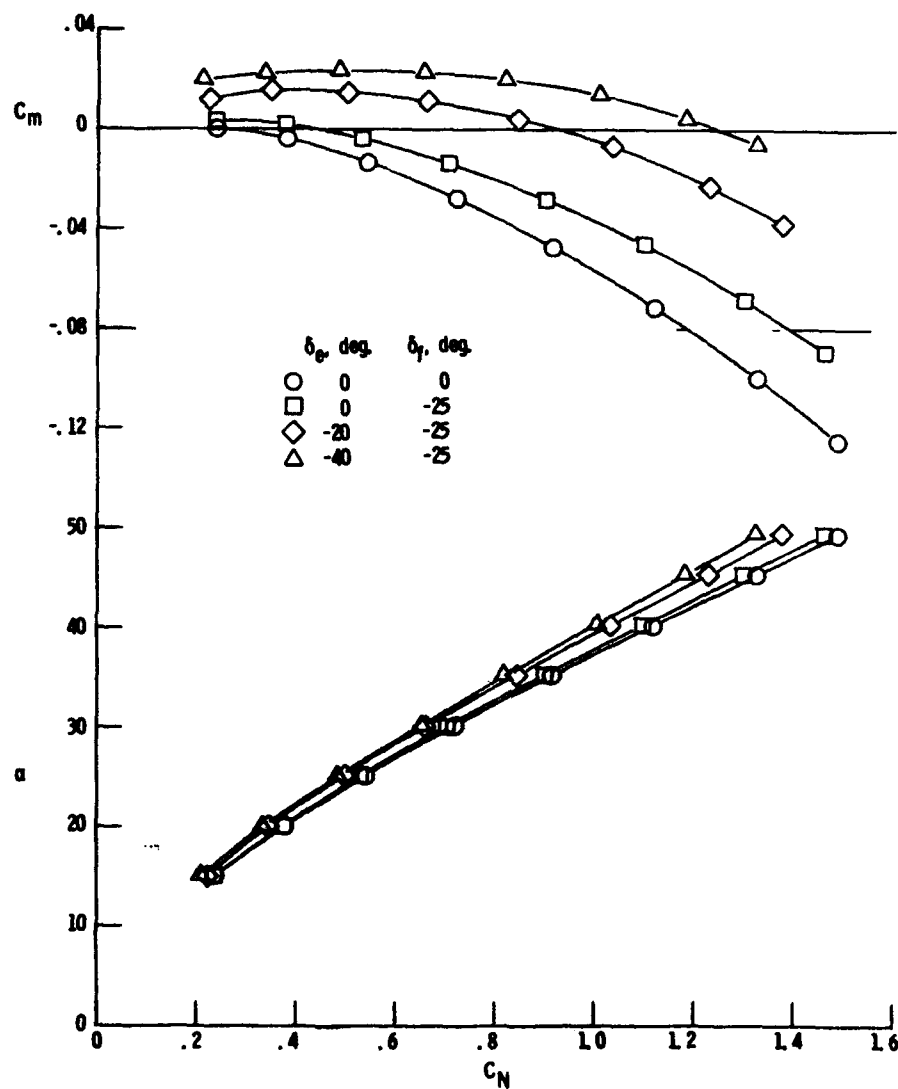


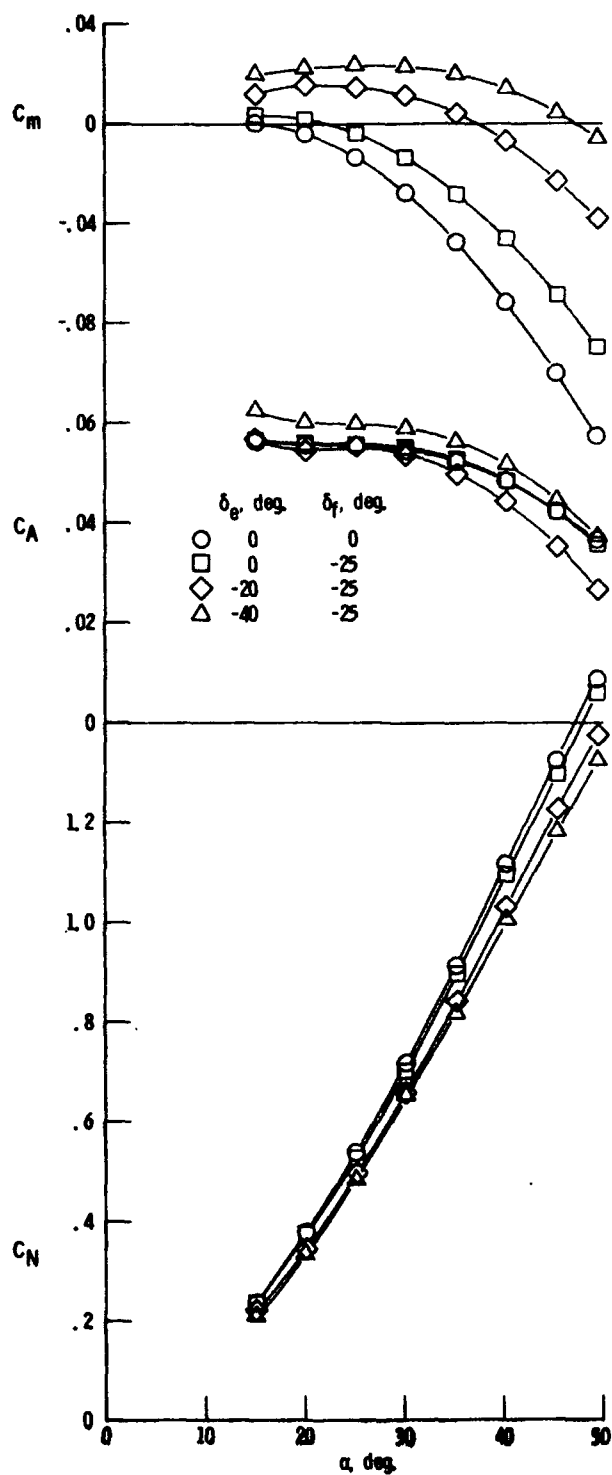
Figure 2 - Sketch of single fin version (dimensions normalized to body reference length).





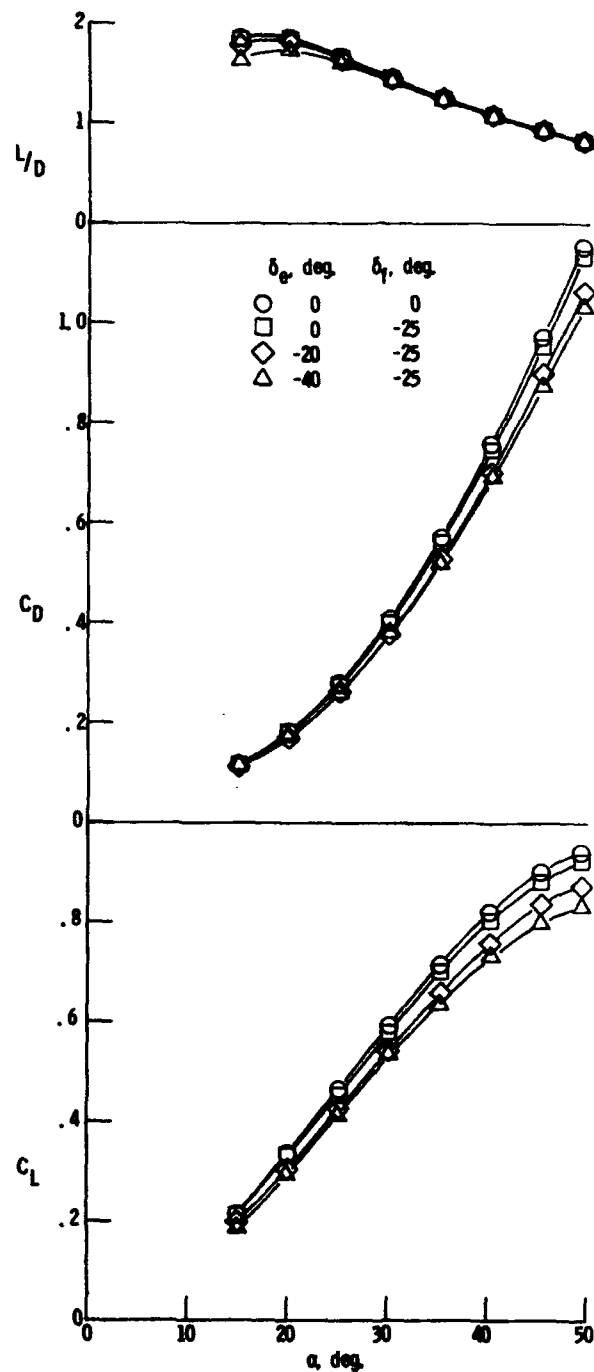
(a) Body axis.

Figure 3 - Elevon and body flap deflection effect on longitudinal aerodynamic characteristics for twin fin version.  $M = 10.3$ .



(b) Body axis.

Figure 3 - Continued.



(c) Stability axis.  
Figure 3. - Concluded.

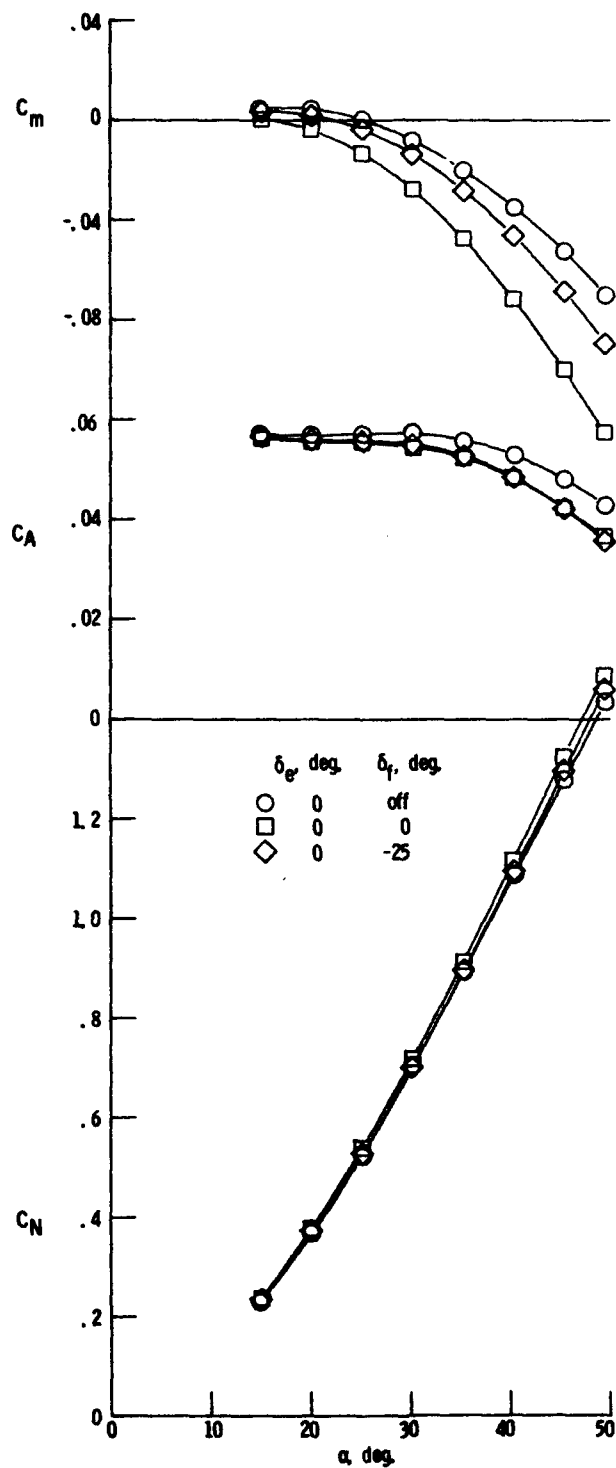


Figure 4 - Body flap deflection effect on longitudinal aerodynamic characteristics for twin fin version. Body axis,  $\delta_e = 0^\circ$ ,  $M = 10.3$ .

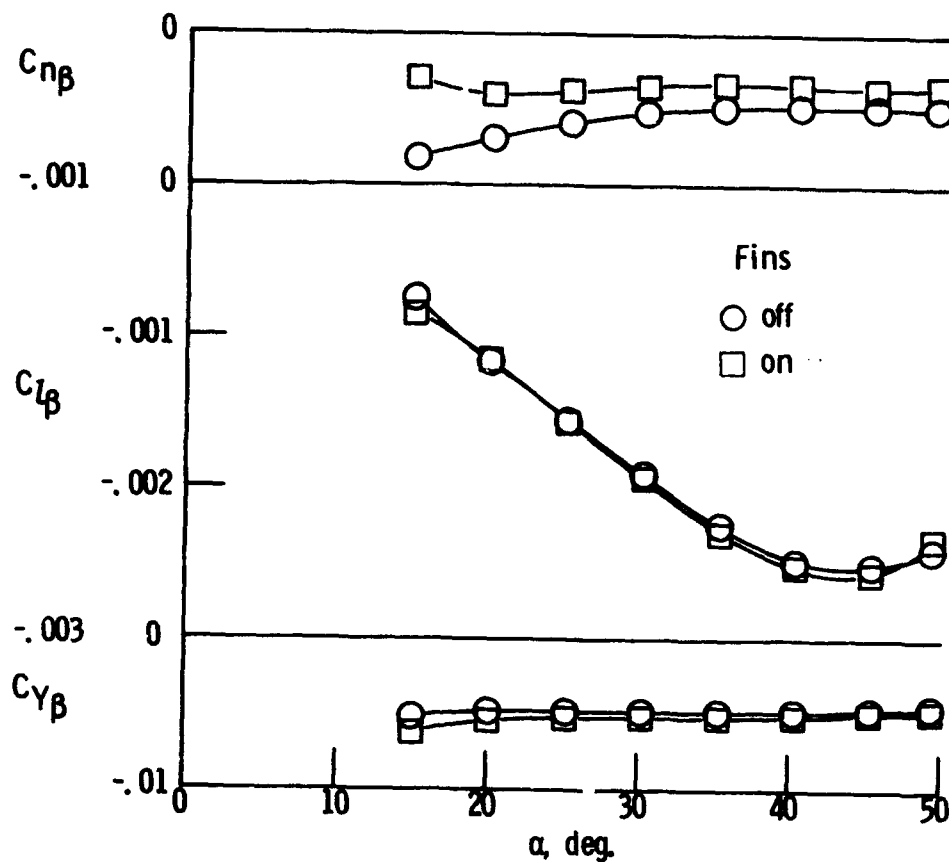


Figure 5. - Dorsal fin effects on lateral-directional stability characteristics on twin fin version,  $\delta_f = 0^\circ$ ,  $\delta_e = 0^\circ$ ,  $M = 10.3$ .

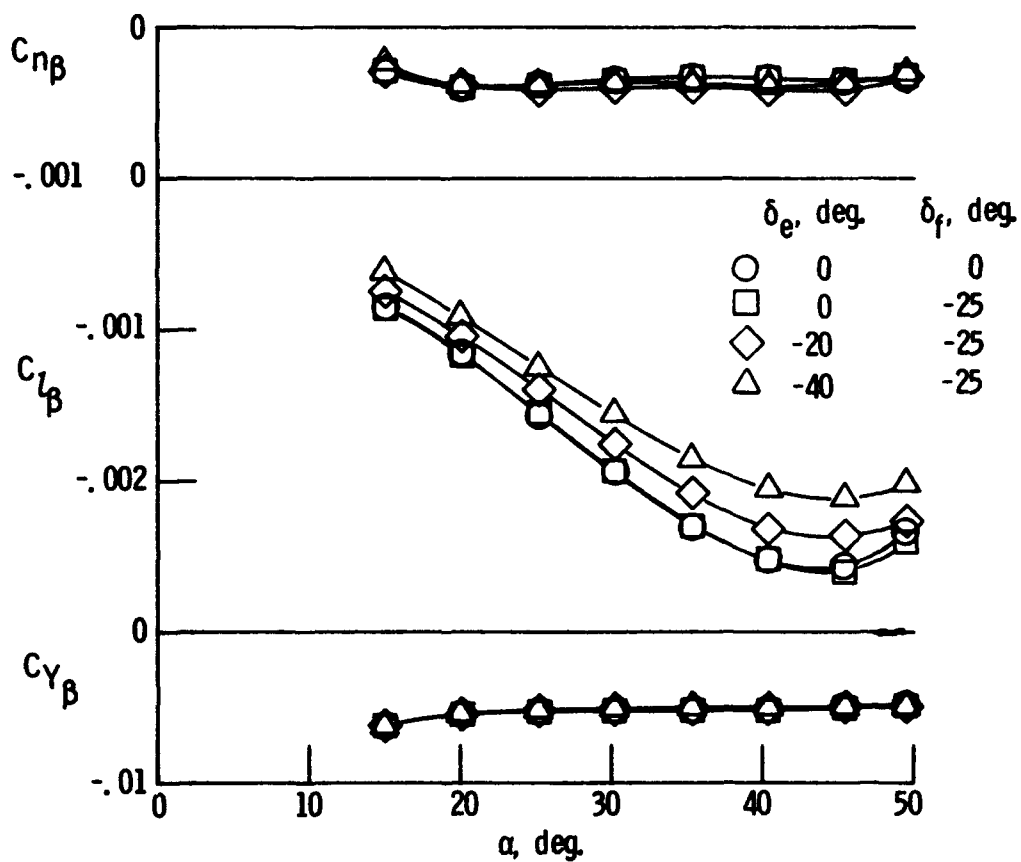


Figure 6. - Elevon and body flap deflection effects on lateral-directional characteristics with 15° rolled out dorsal fins on twin fin version.  $M = 10.3$

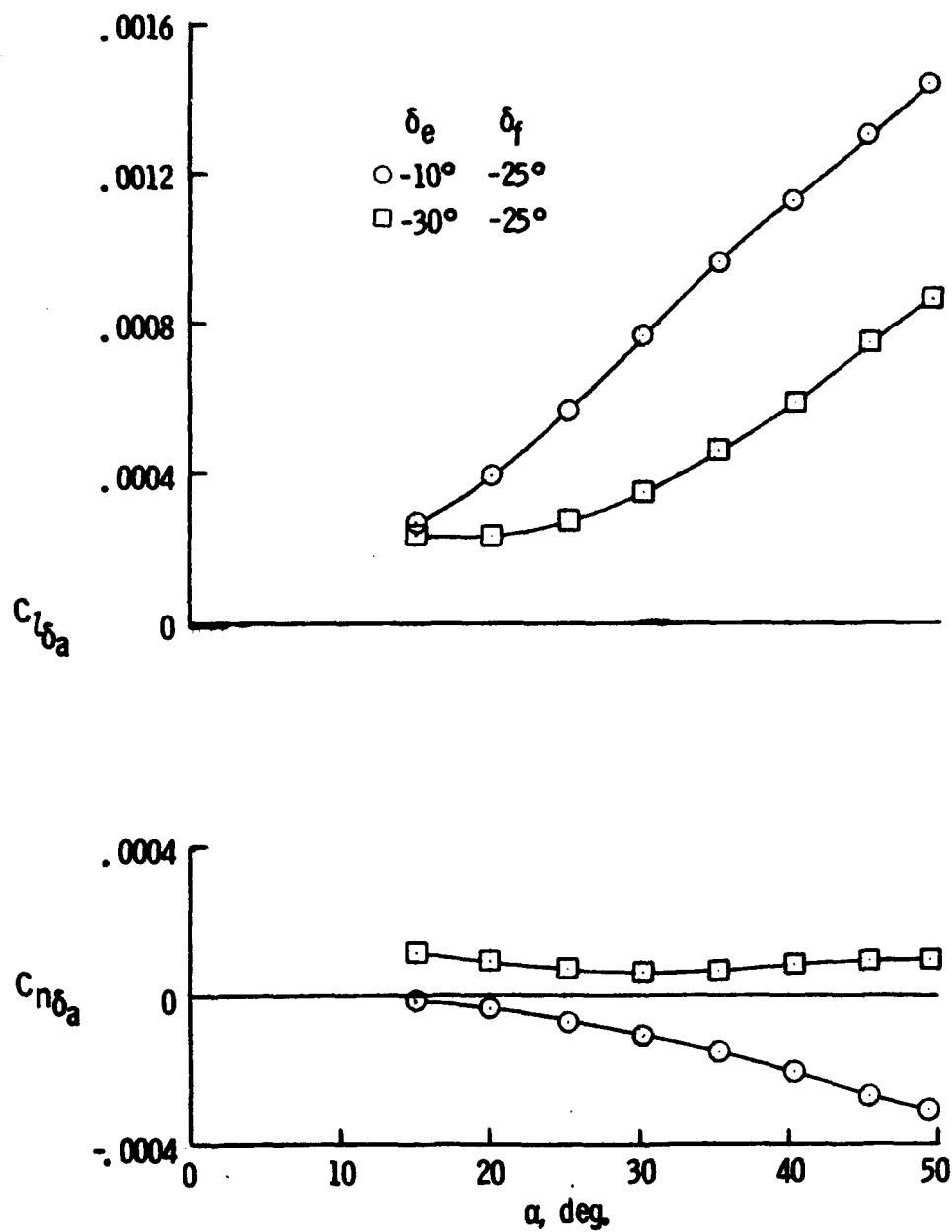
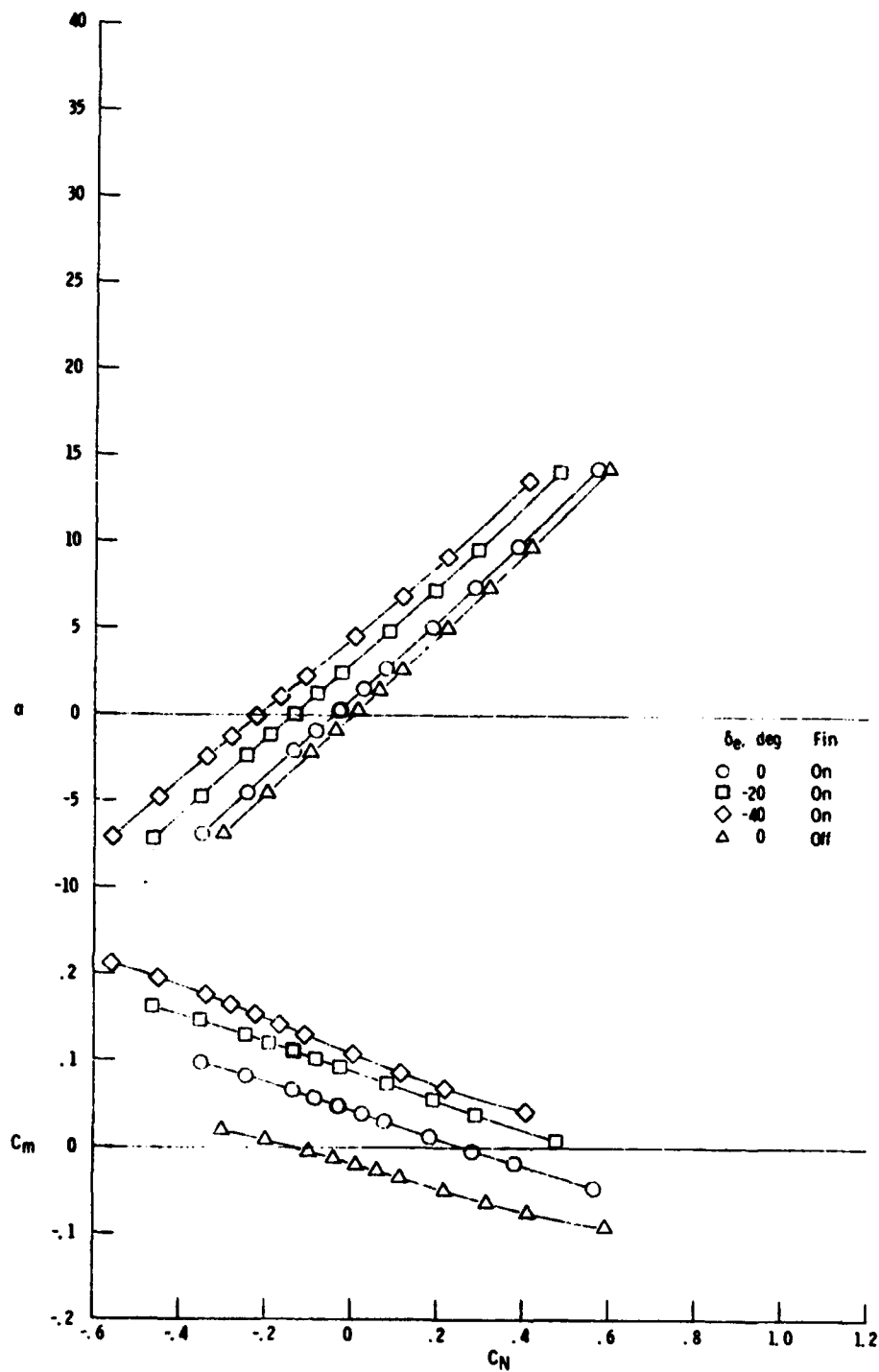


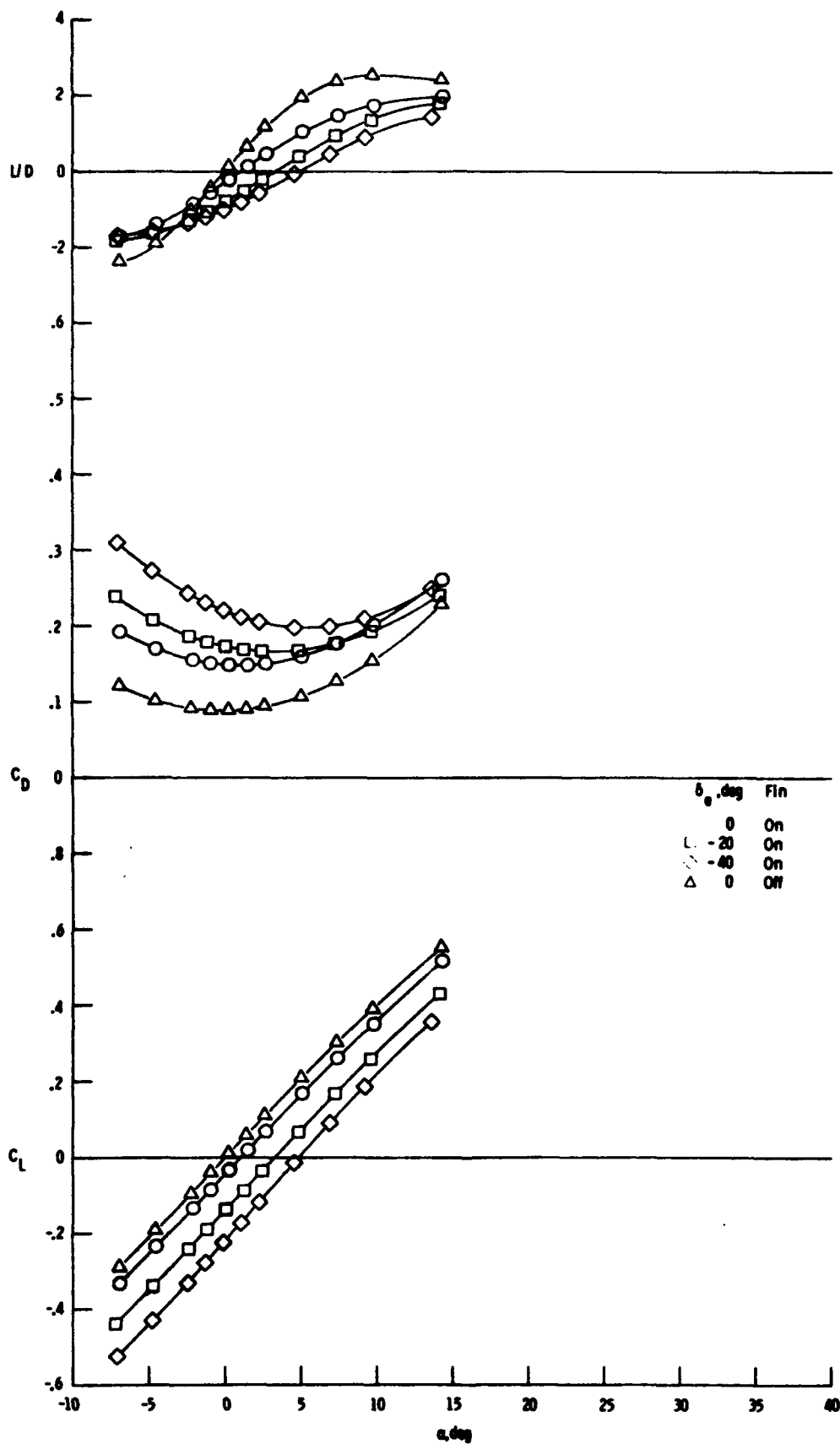
Figure 7. - Roll control effectiveness on twin fin version,  $\delta_a = 10^\circ$ .  $M = 10.3$ .



(a)  $M = 1.6$

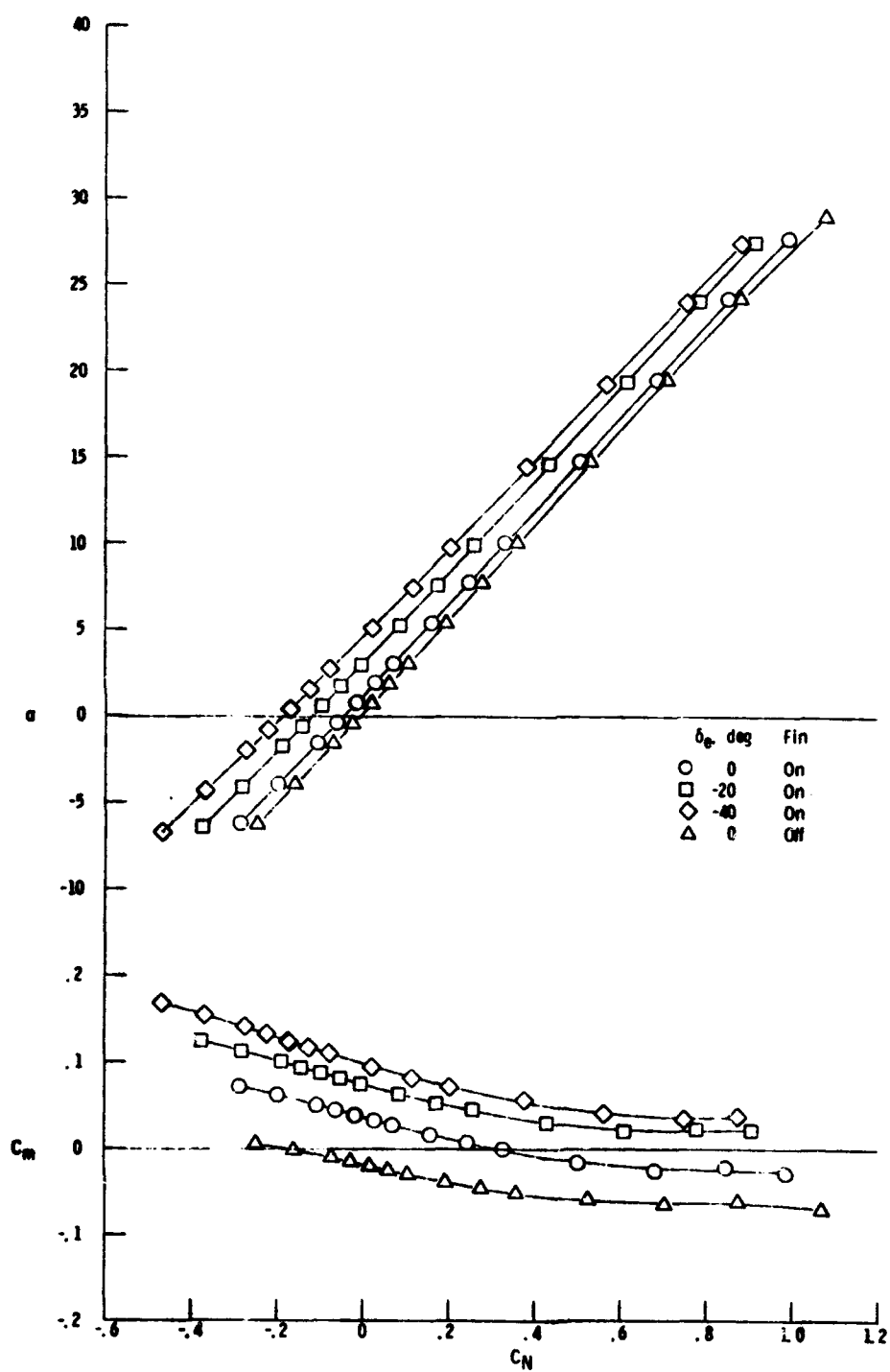
Figure 8 - Elevon deflection effect on longitudinal stability characteristics of single fin version, planform fillet off, rudder flared  $30^\circ$ ,  $\delta_f = 0^\circ$





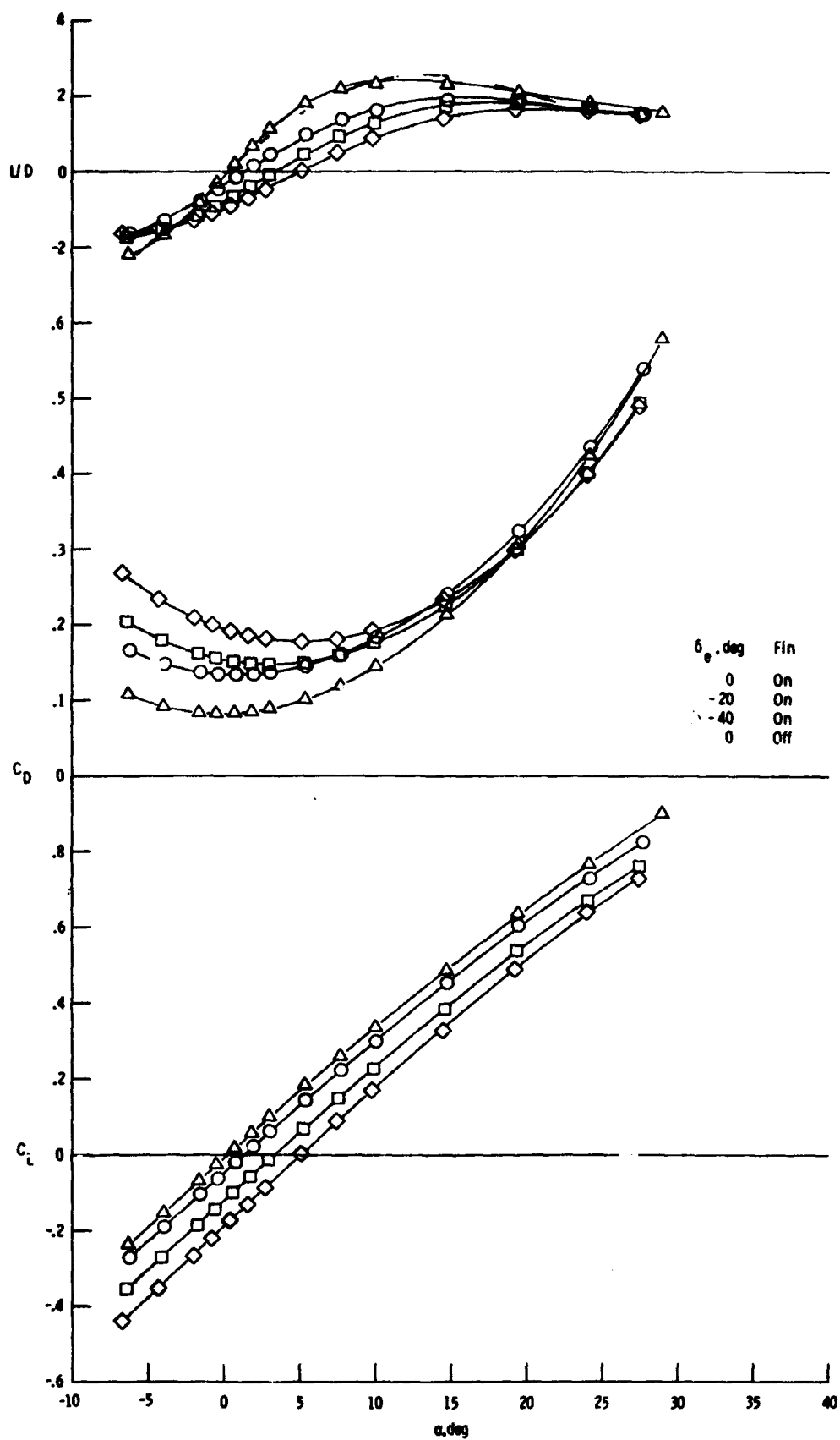
(a) Concluded.

Figure 8. - Continued.

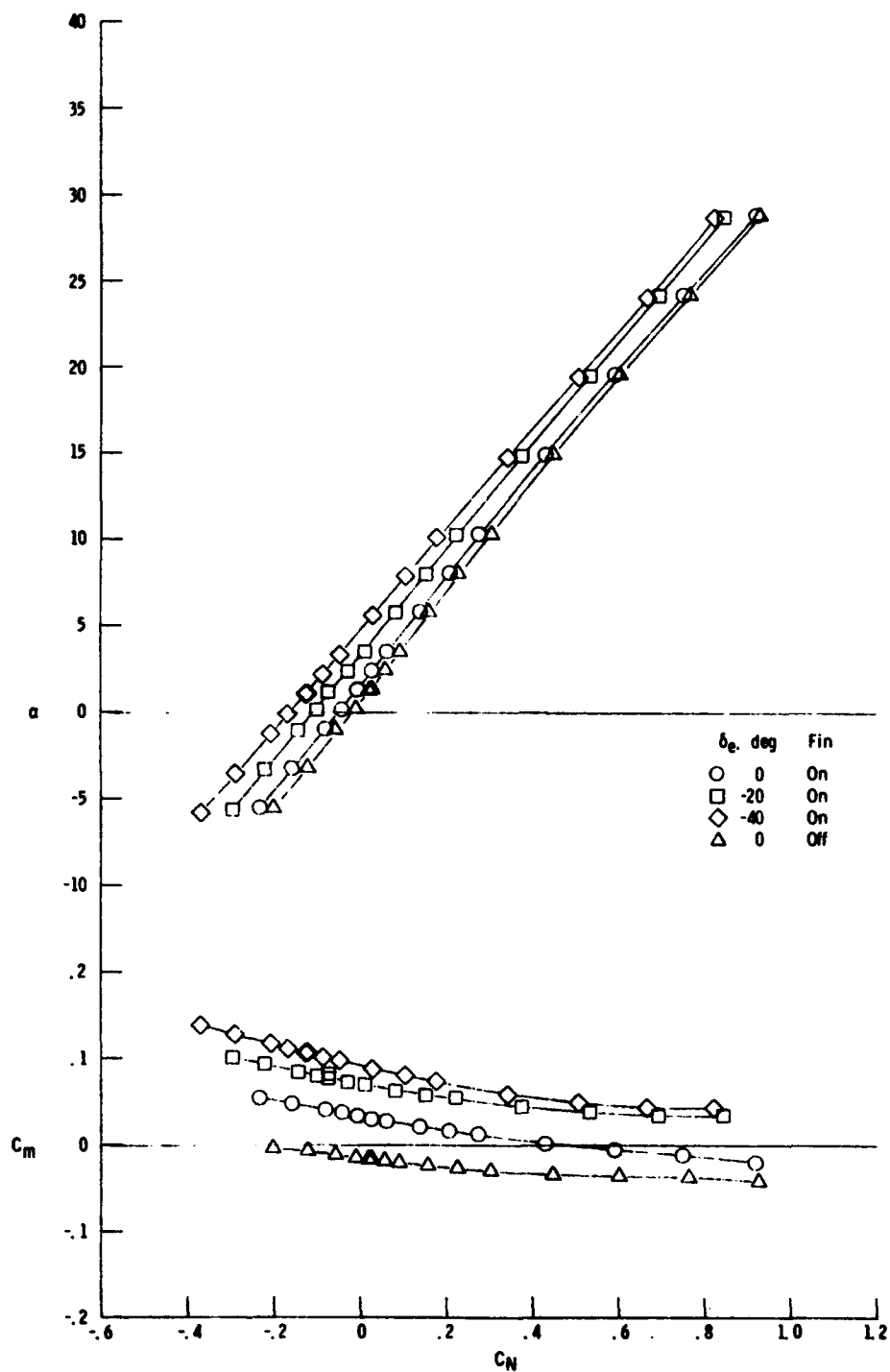


(b)  $M = 1.9$

Figure 8. - Continued.

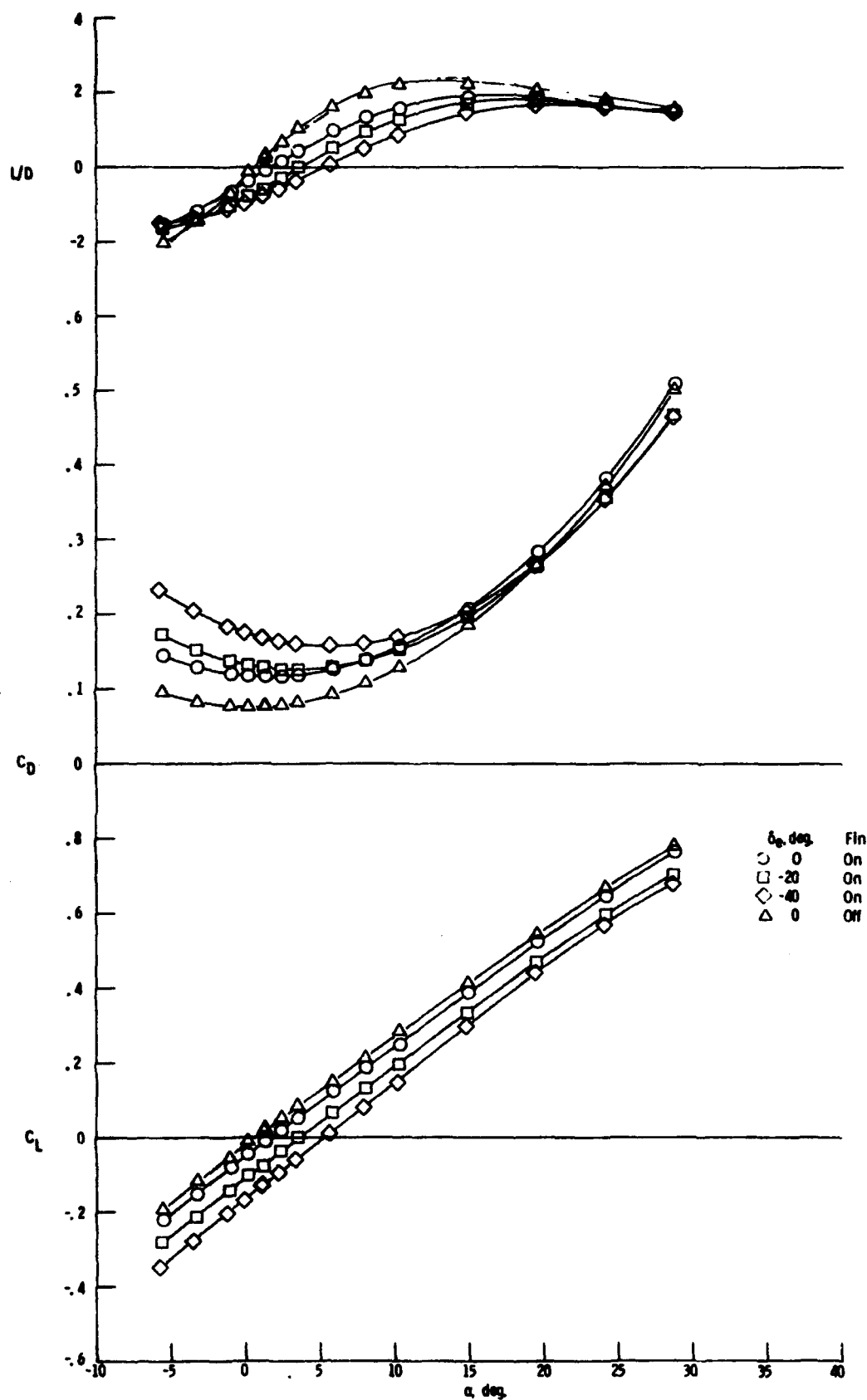


(b) Concluded.  
Figure 8. - Continued.



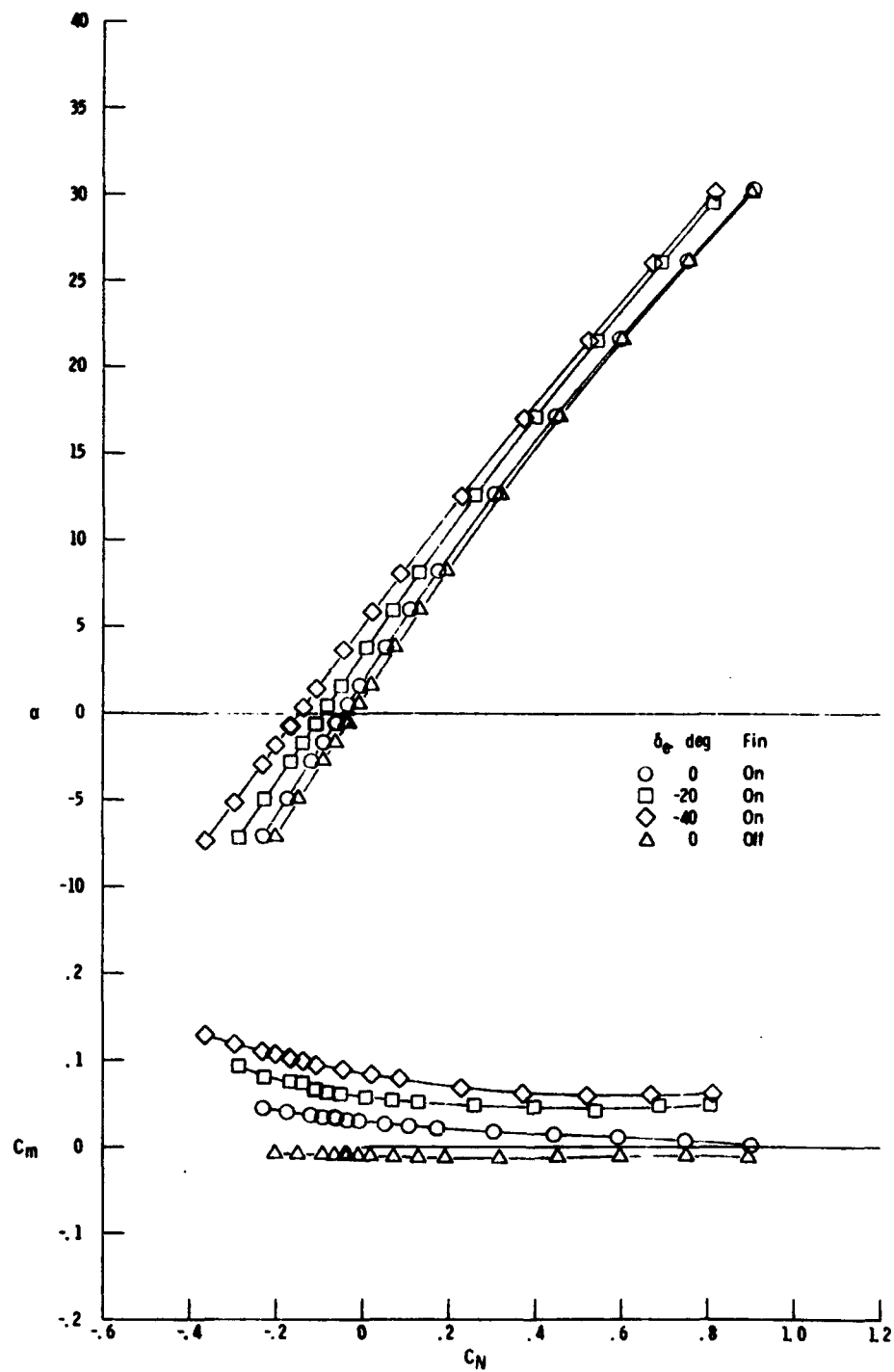
(c)  $M = 2.36$

Figure 8 - Continued.



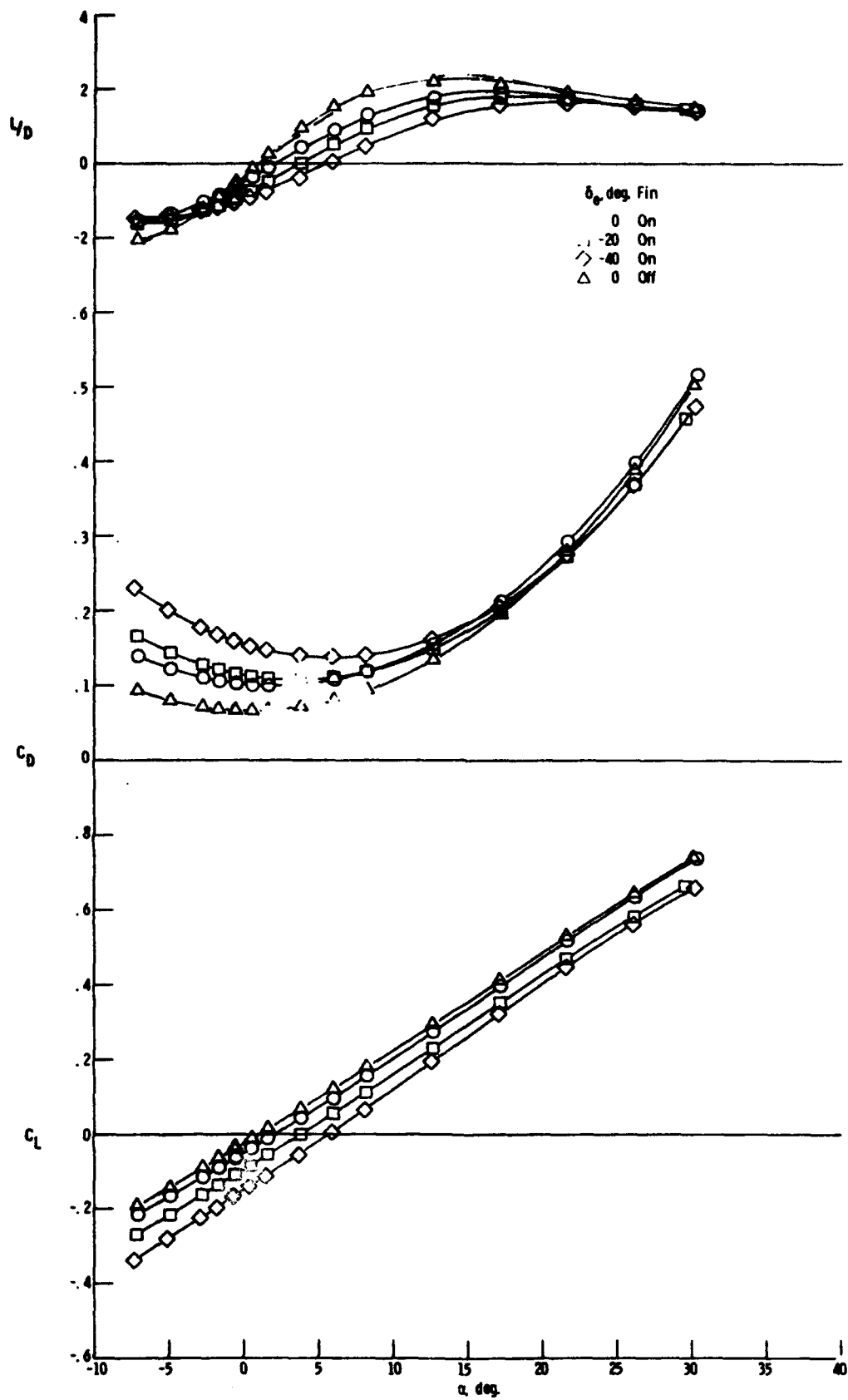
(c) Concluded.

Figure 8 - Continued.



(d)  $M = 2.86$

Figure 8 - Continued.



(d) Concluded.

Figure 8 - Concluded.

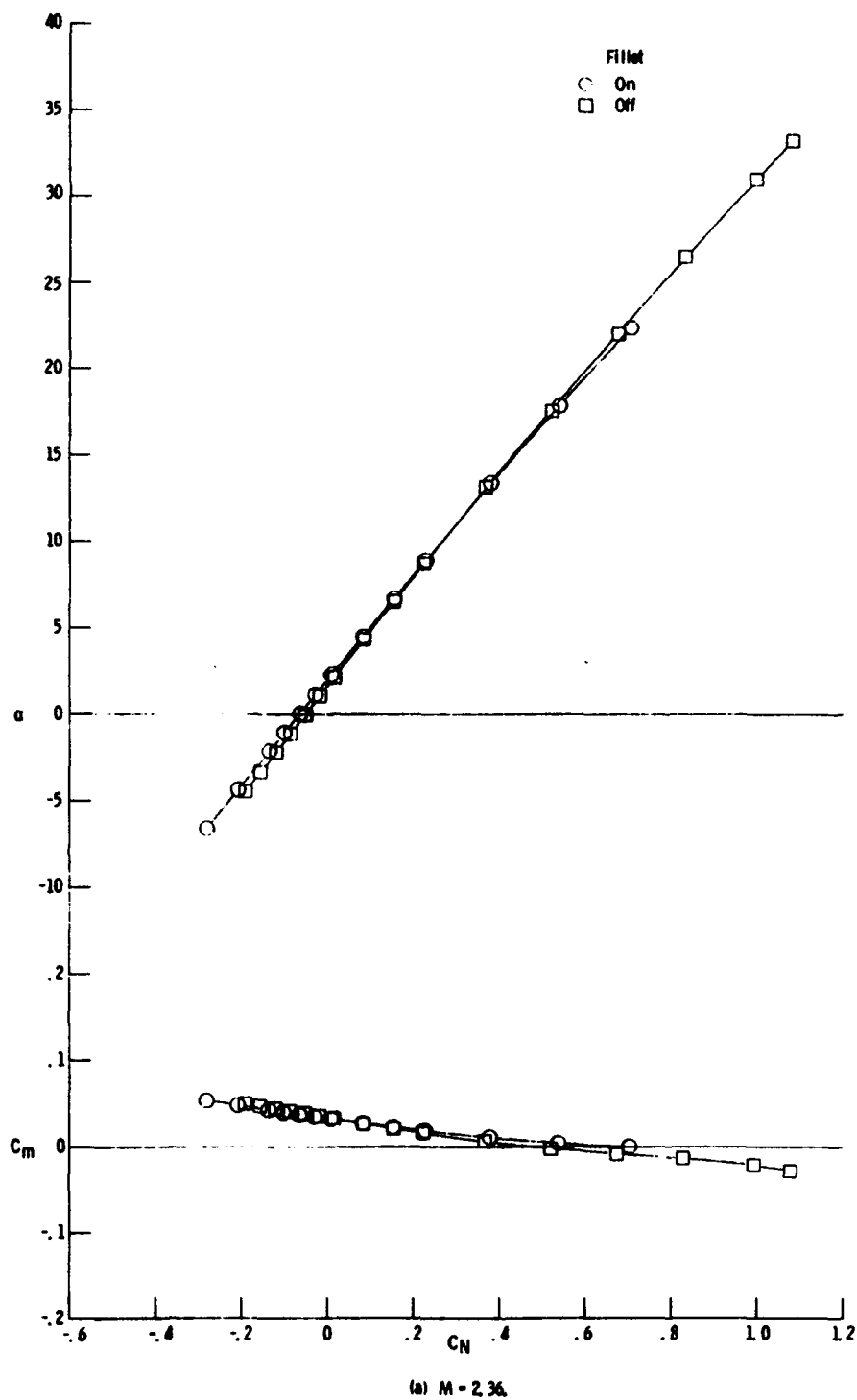
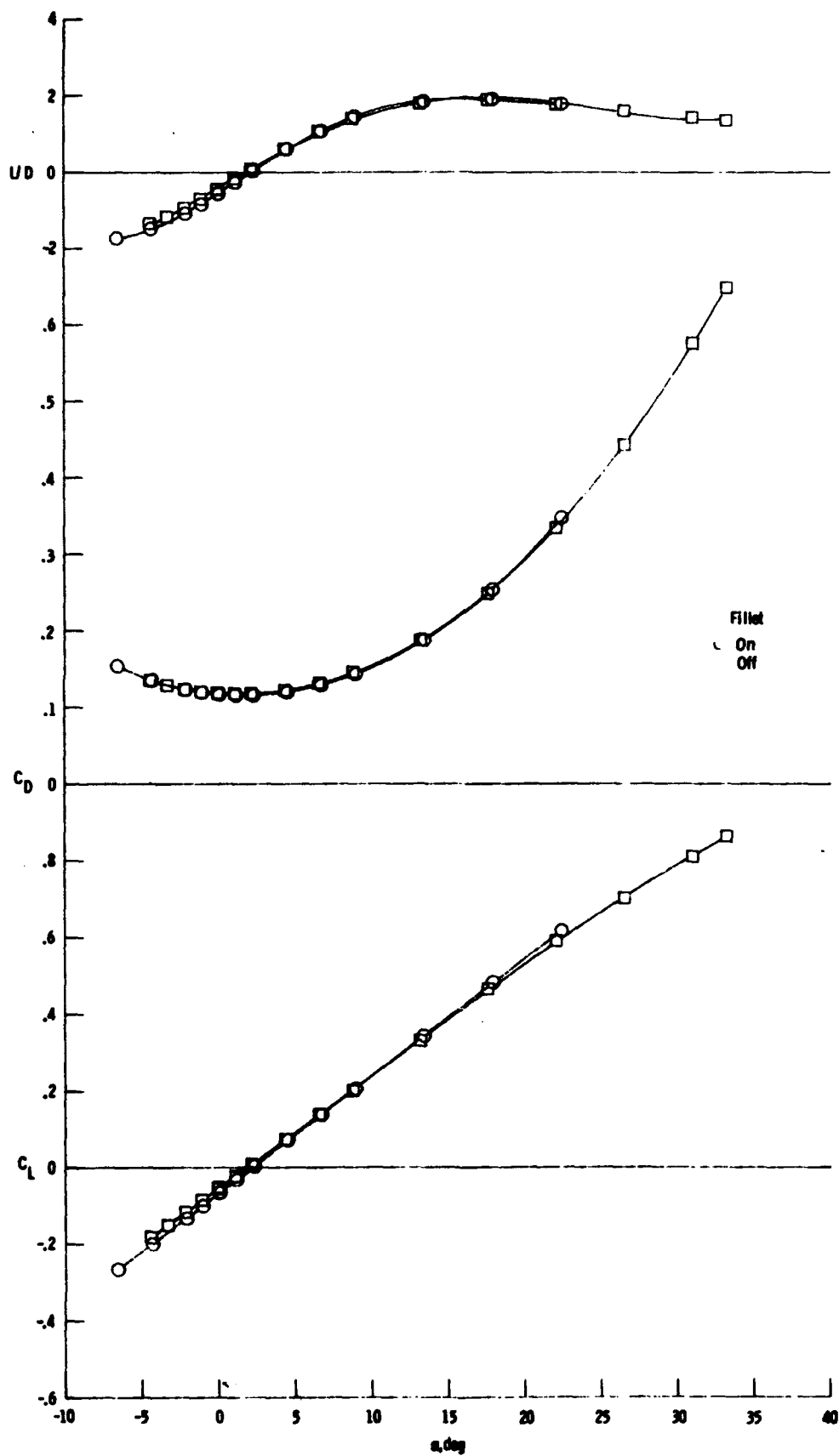
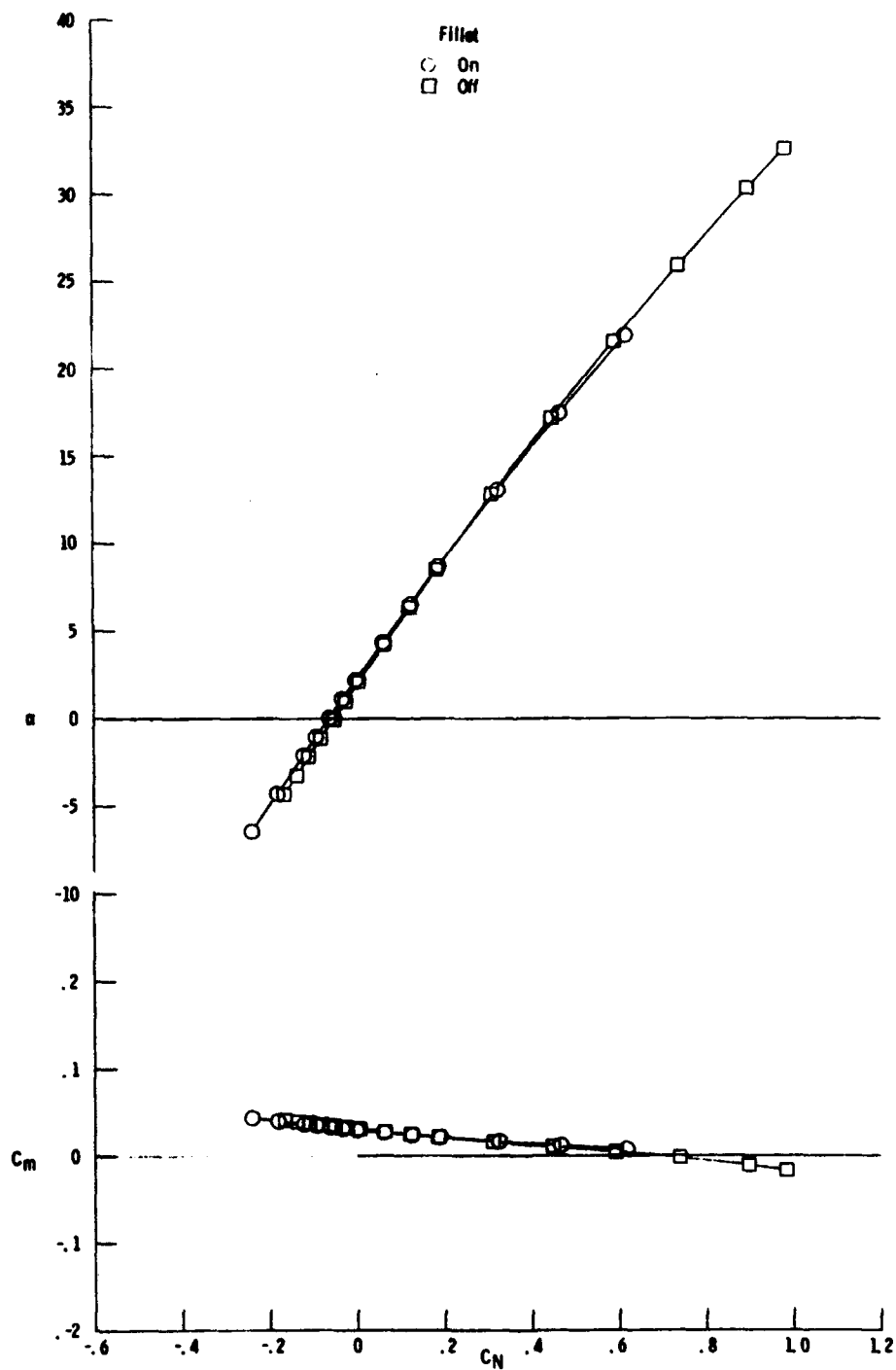


Figure 9. - Planform fillet effect on longitudinal stability characteristics of single fin version, rudder flared  $30^\circ$ ,  $\delta_\theta = \delta_\gamma = 0^\circ$

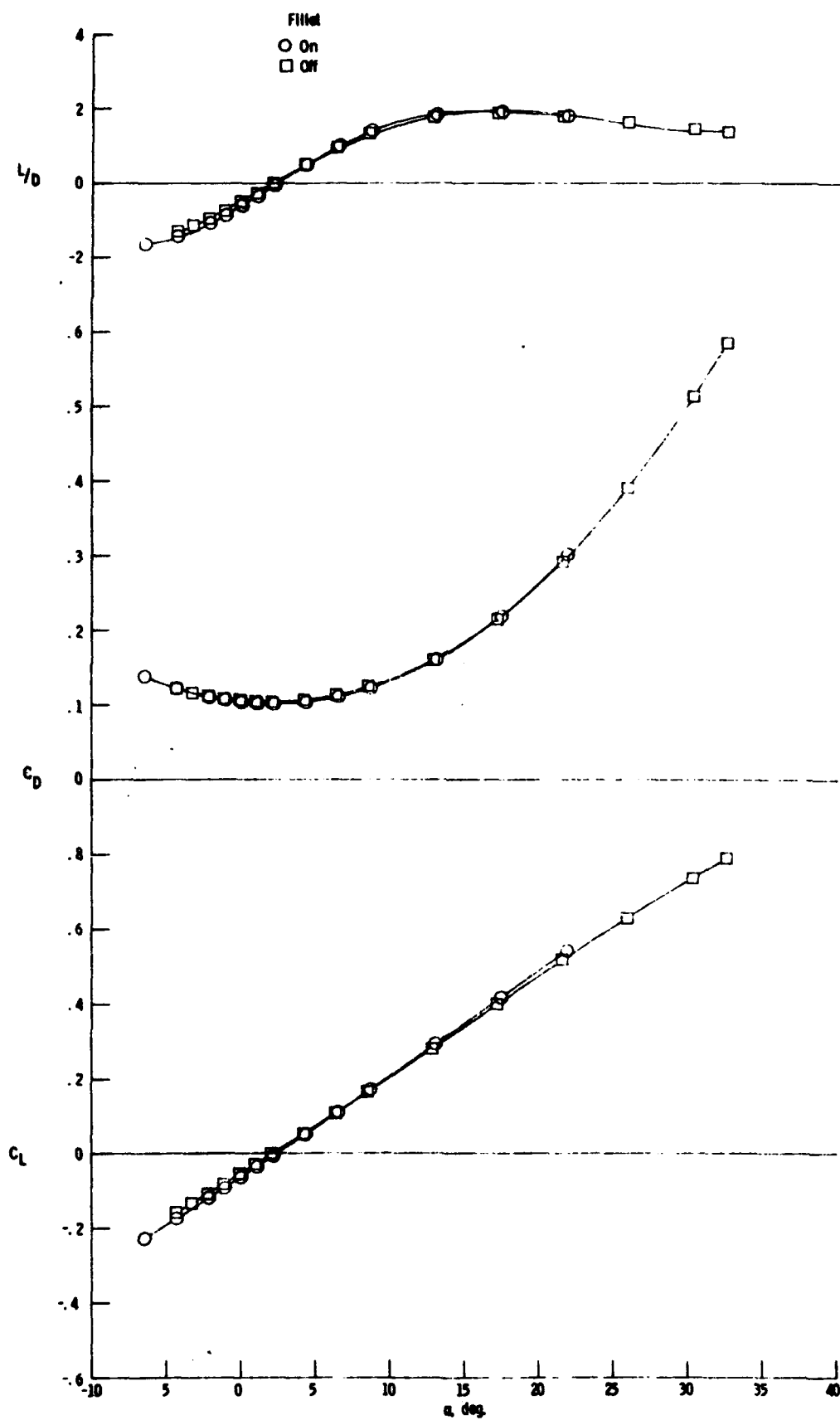




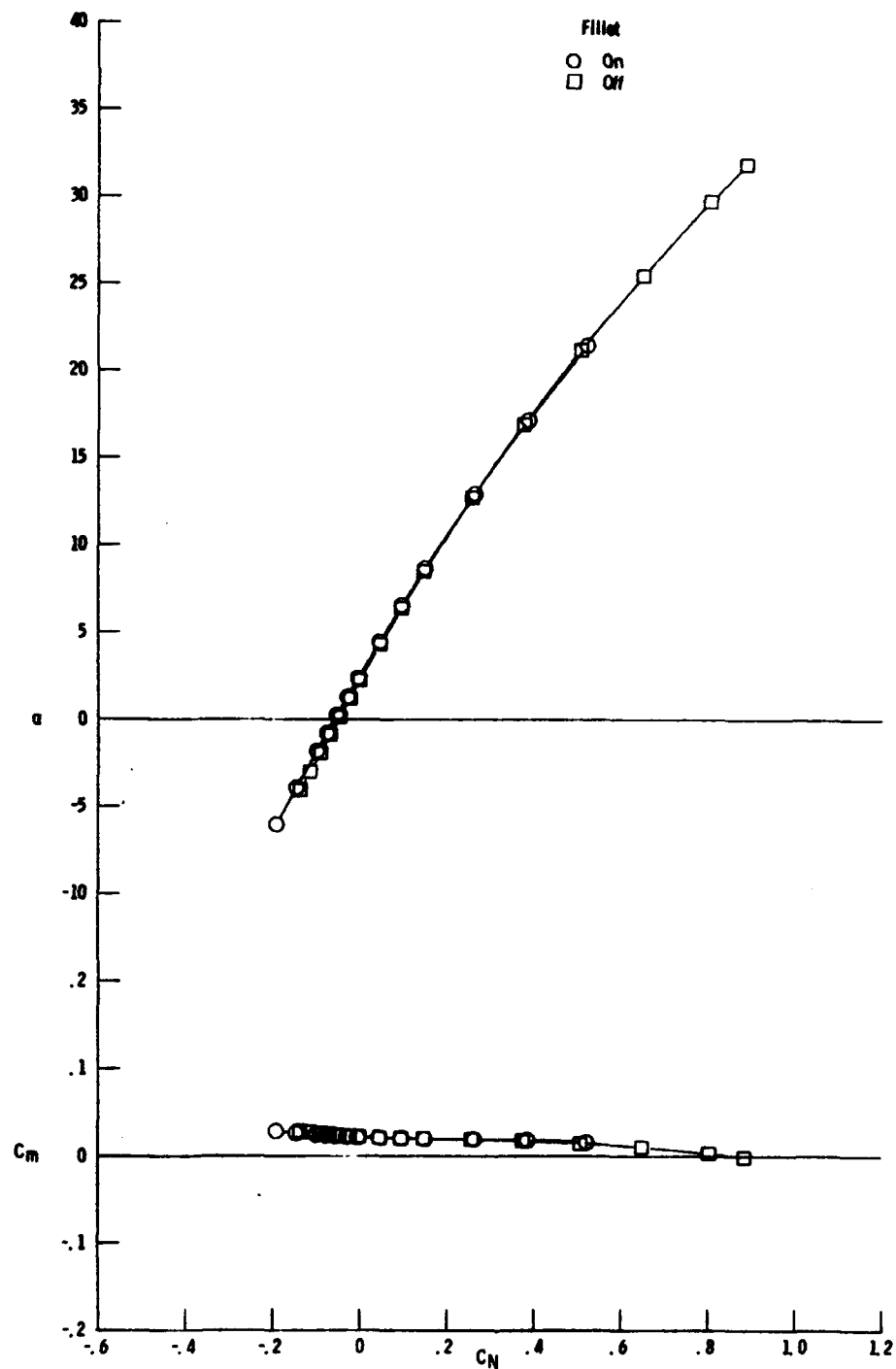
(a) Concluded.  
Figure 9.- Continued.



(b)  $M = 2.86$   
Figure 9. - Continued.

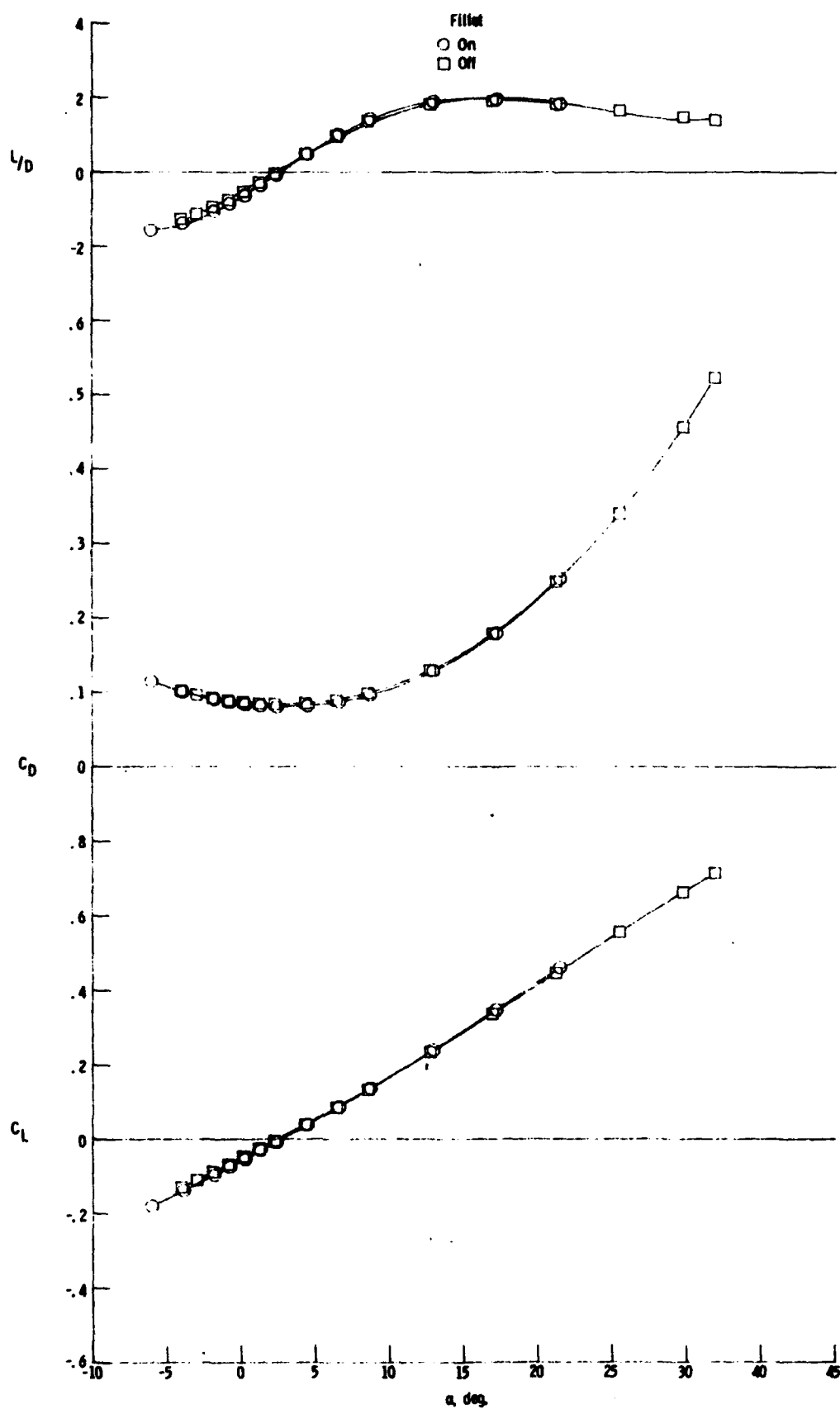


(b) Concluded.  
 Figure 9. - Continued.

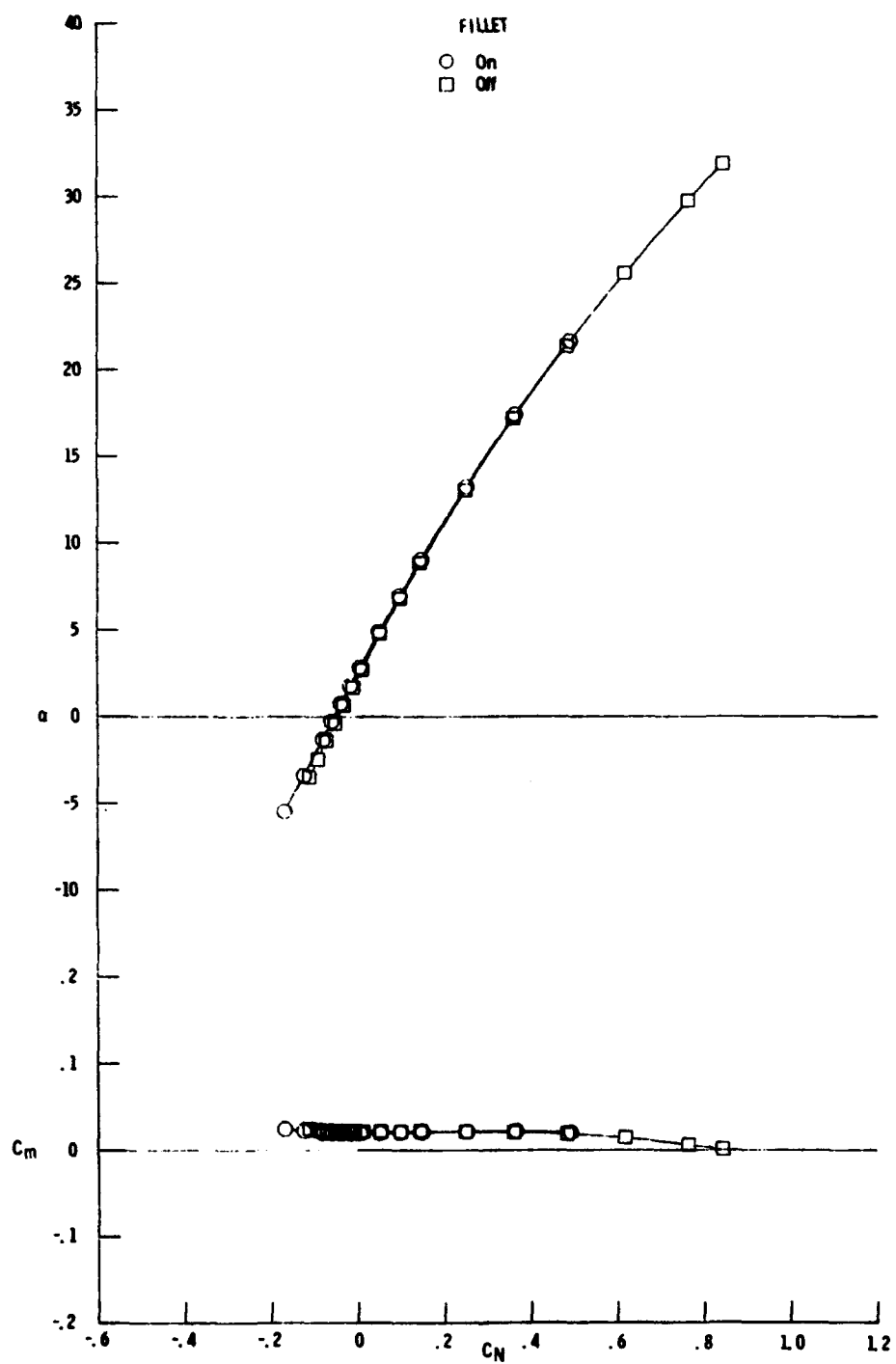


(c)  $M = 3.96$

Figure 9. - Continued.

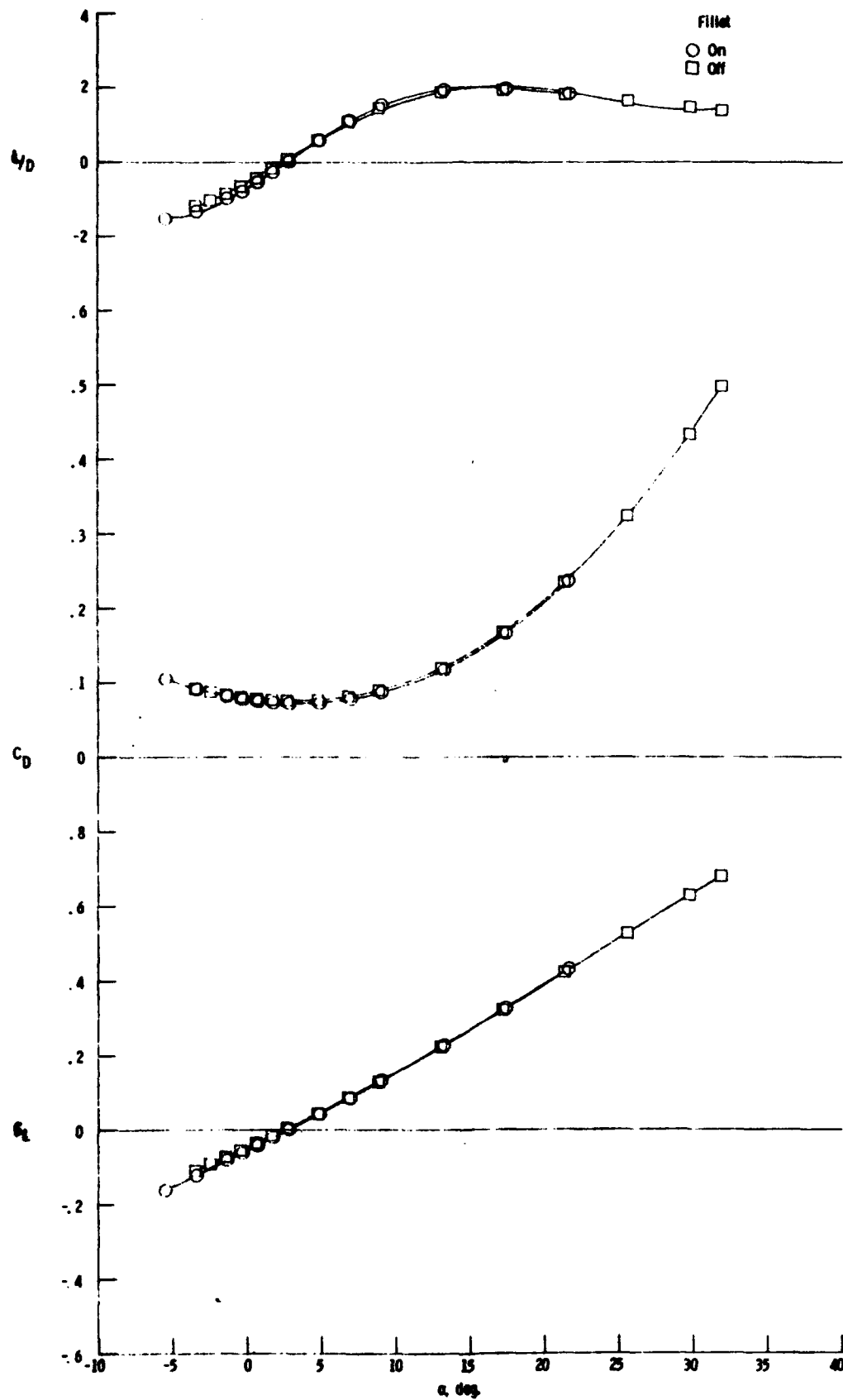


(c) Concluded  
 Figure 9. - Continued.



(d)  $M = 4.63$

Figure 9. - Continued.



(d) Concluded.  
Figure 9. - Concluded

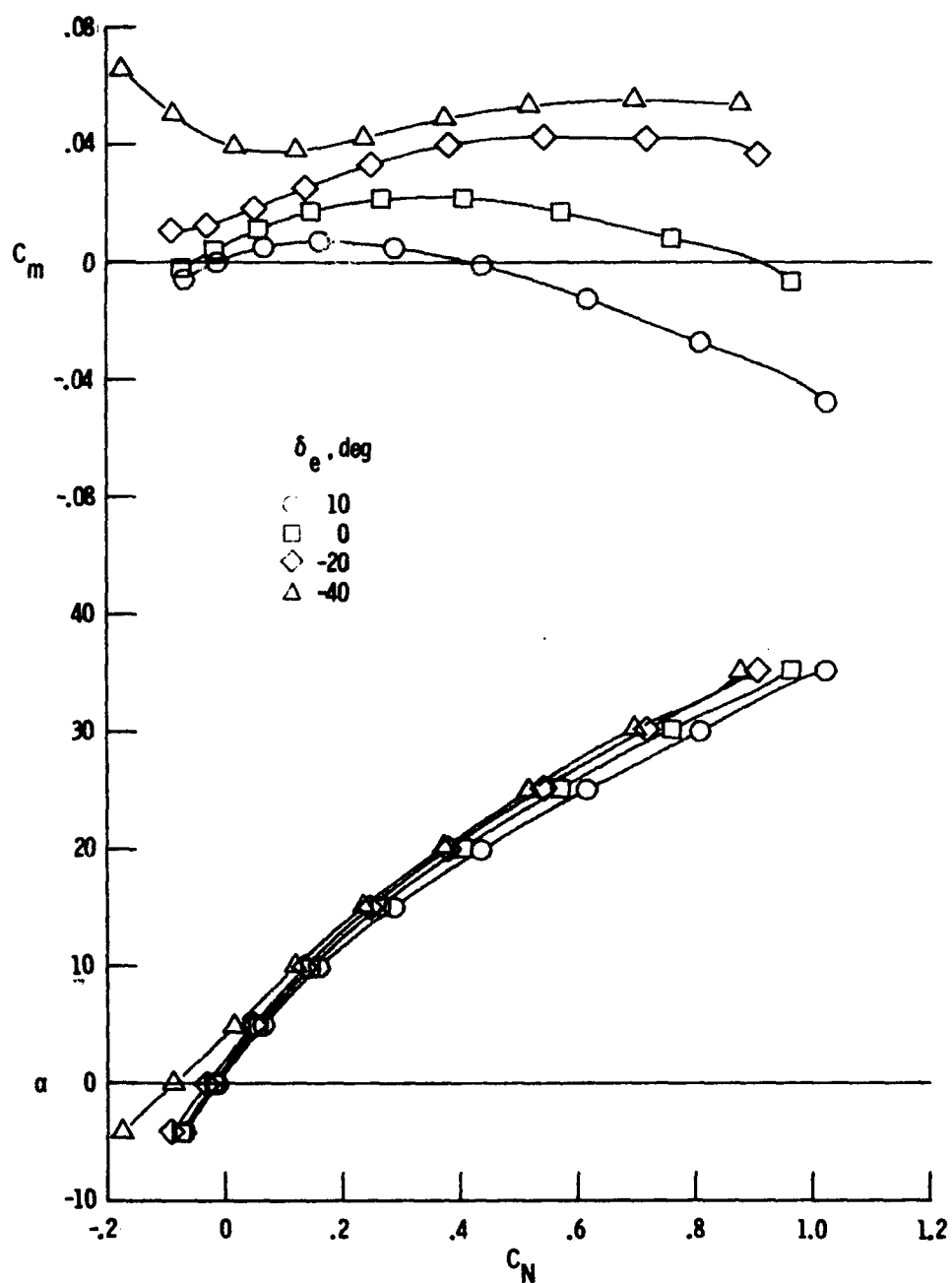


Figure 10. - Elevon deflection on longitudinal aerodynamic characteristics on single fin version, planform fillet off, fin on, rudder unflared, straight sting,  $\delta_f = 0^\circ$ ,  $M = 10.3$ .



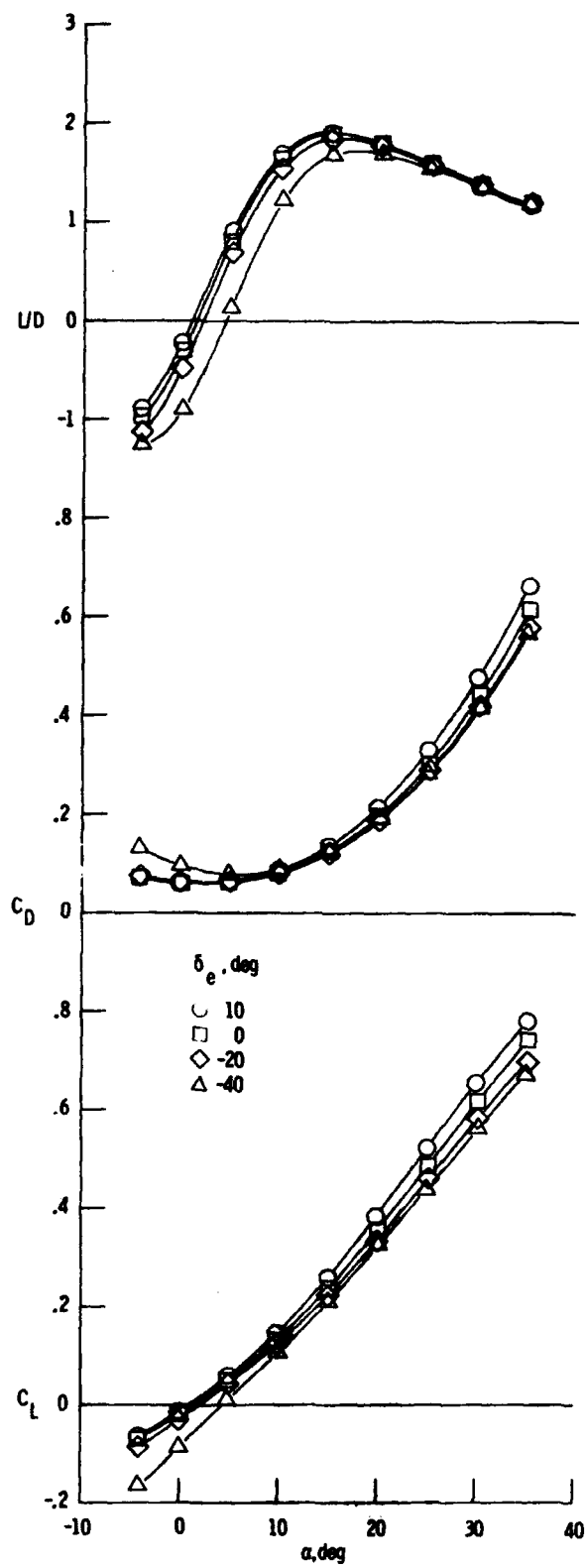


Figure 10. - Concluded.

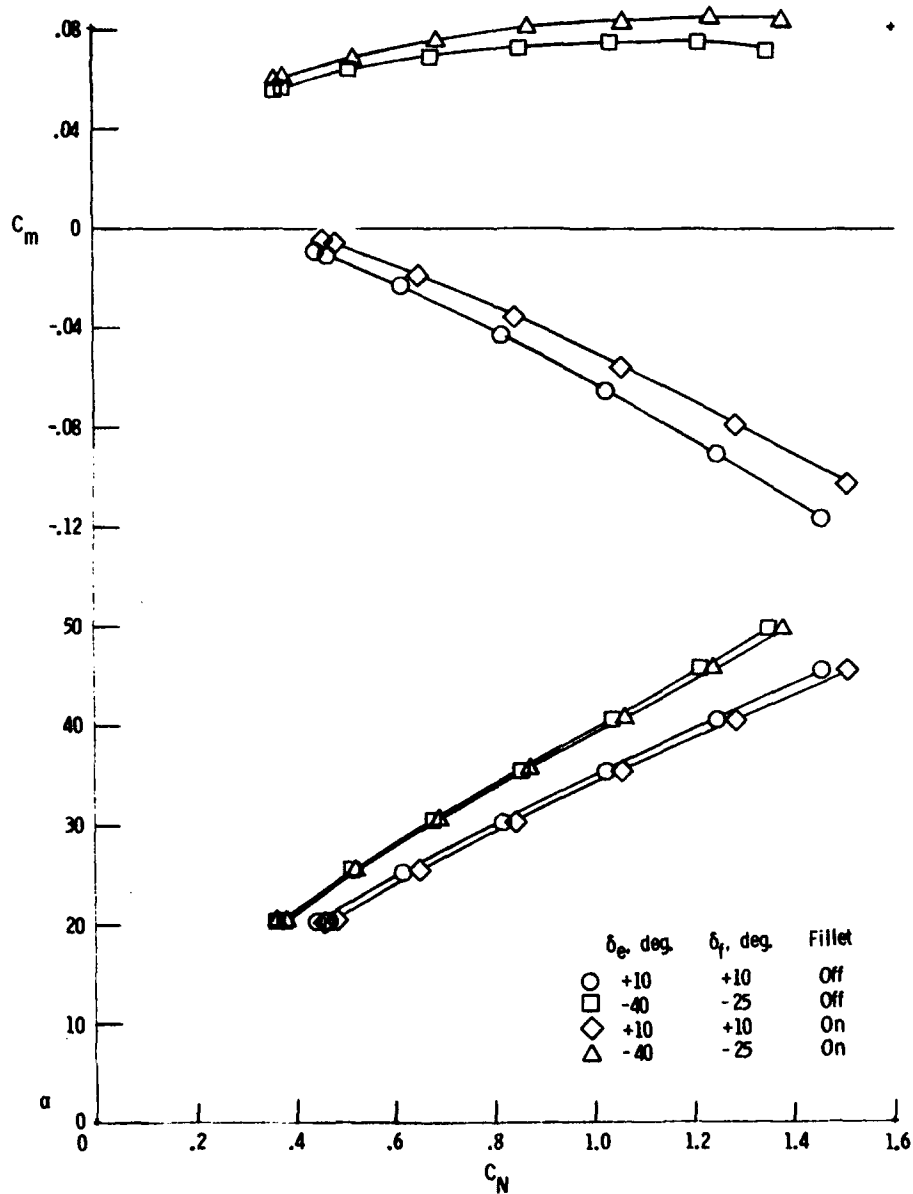


Figure 11. - Elevon and body flap deflection and planform fillet effect on longitudinal aerodynamic characteristics on single fin version, without center fin, on bent sting, at  $M = 10.3$ .

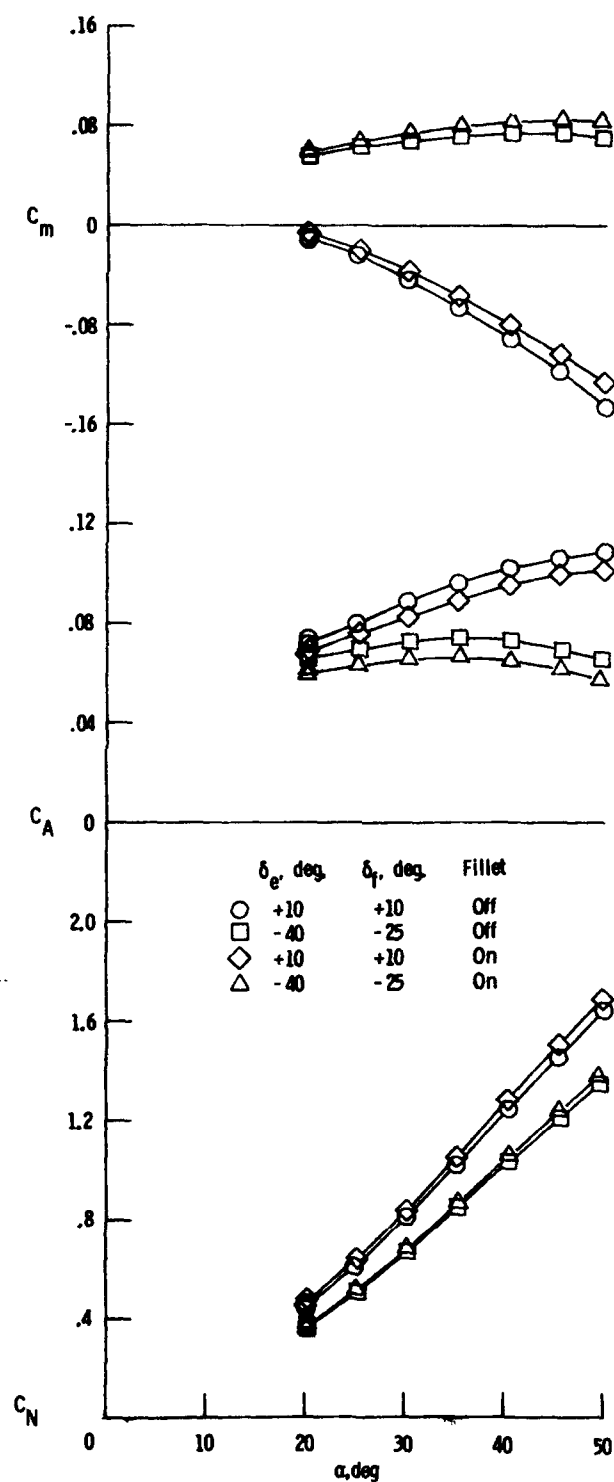


Figure 11. - Continued.

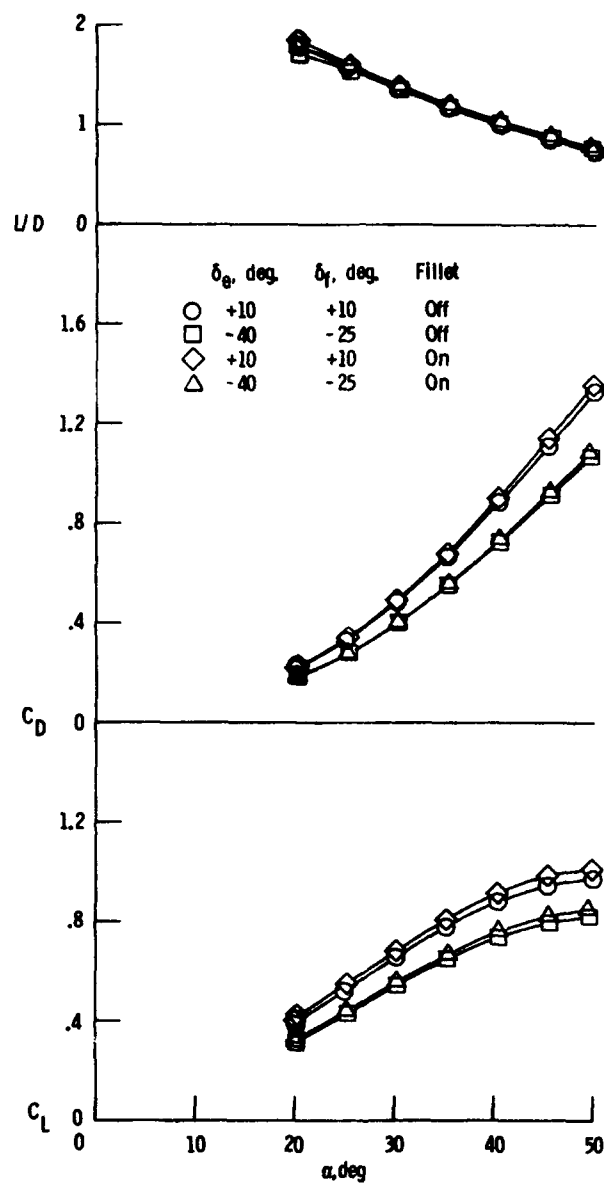


Figure 11. - Concluded.

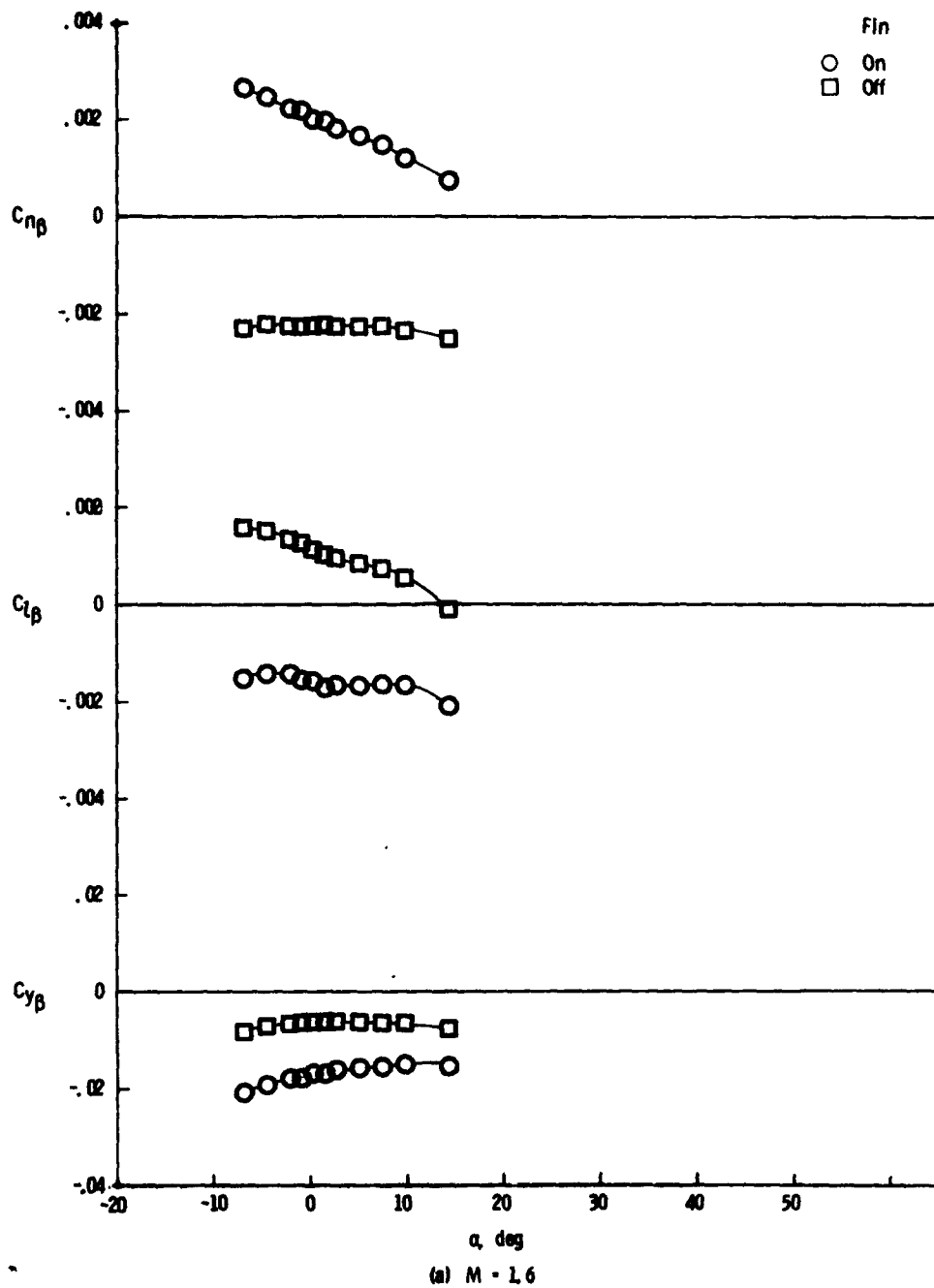
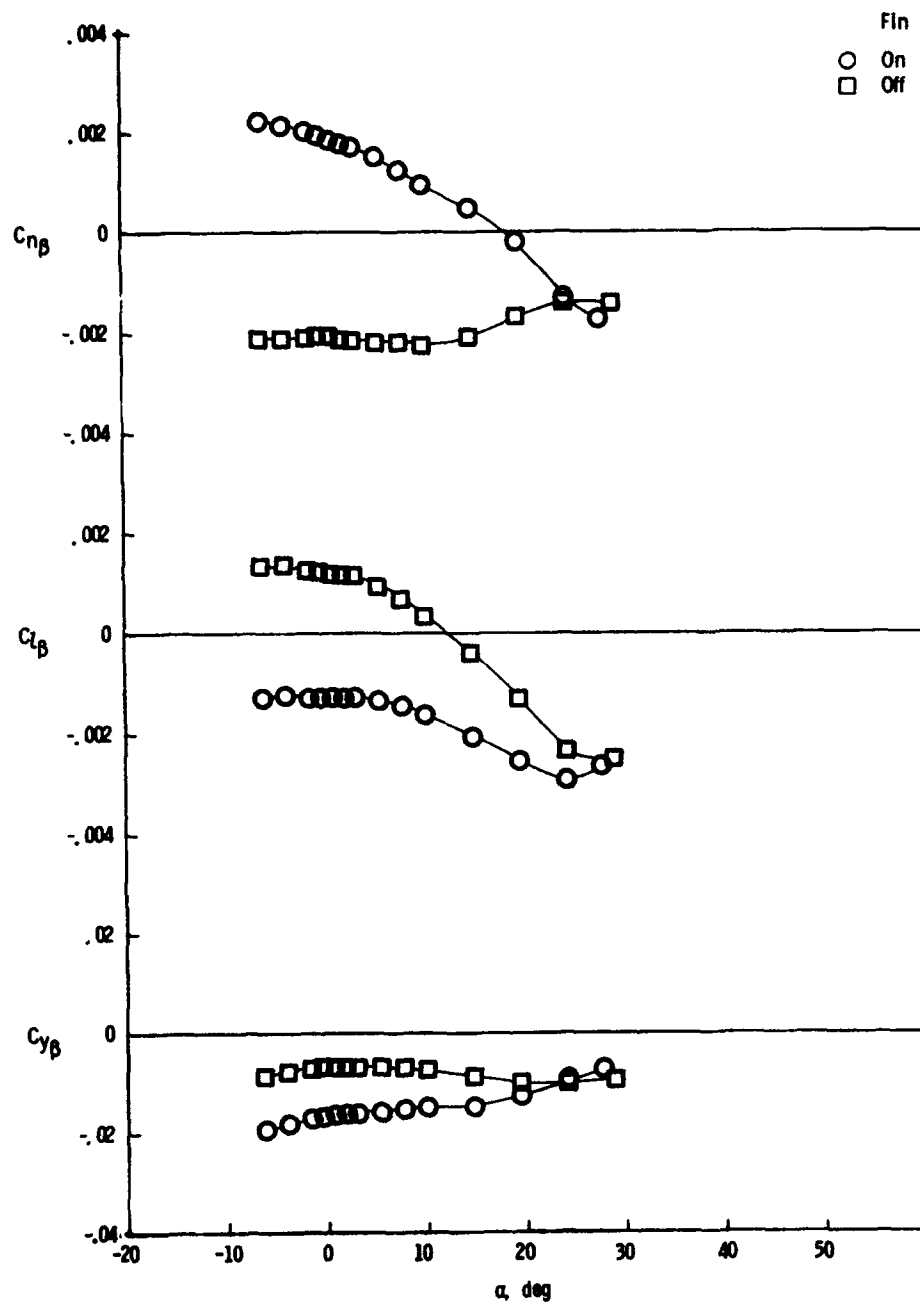
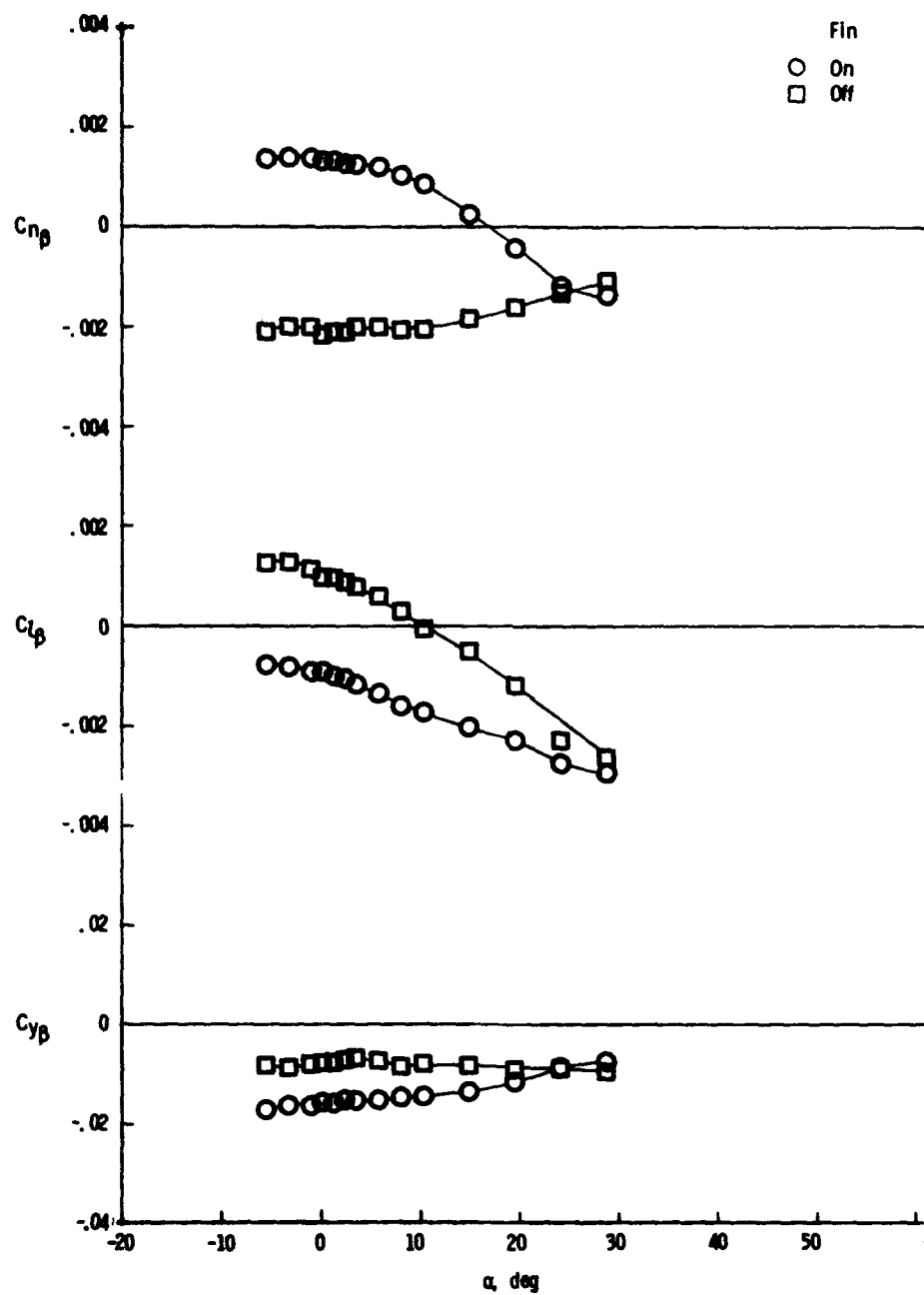


Figure 12 - Effect of center fin (flared rudder) on lateral-directional stability characteristics of single fin version, fillet off,  $\delta_a = \delta_r = 0^\circ$

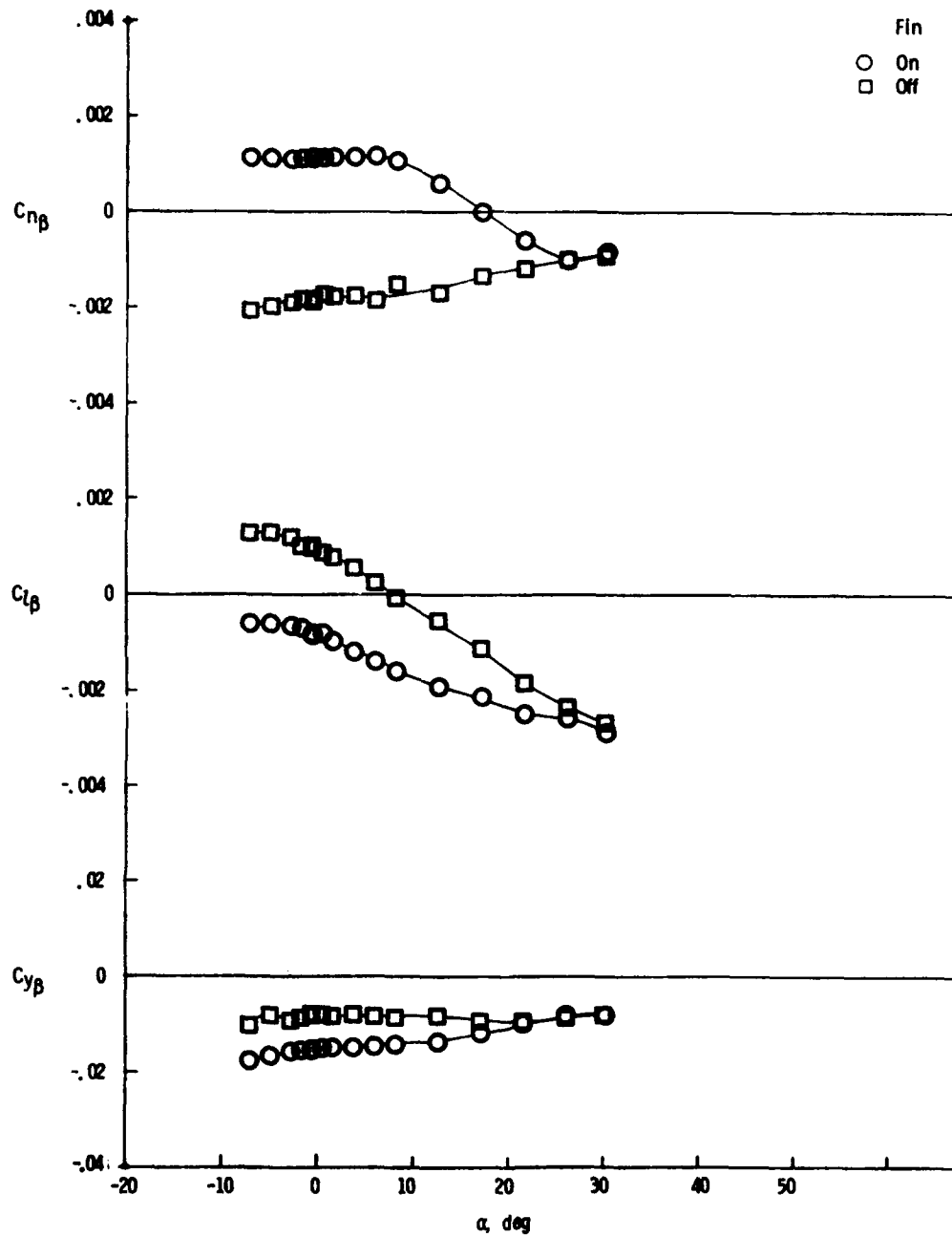


(b)  $M = 1.9$   
Figure 12 - Continued.



(c)  $M = 2.36$

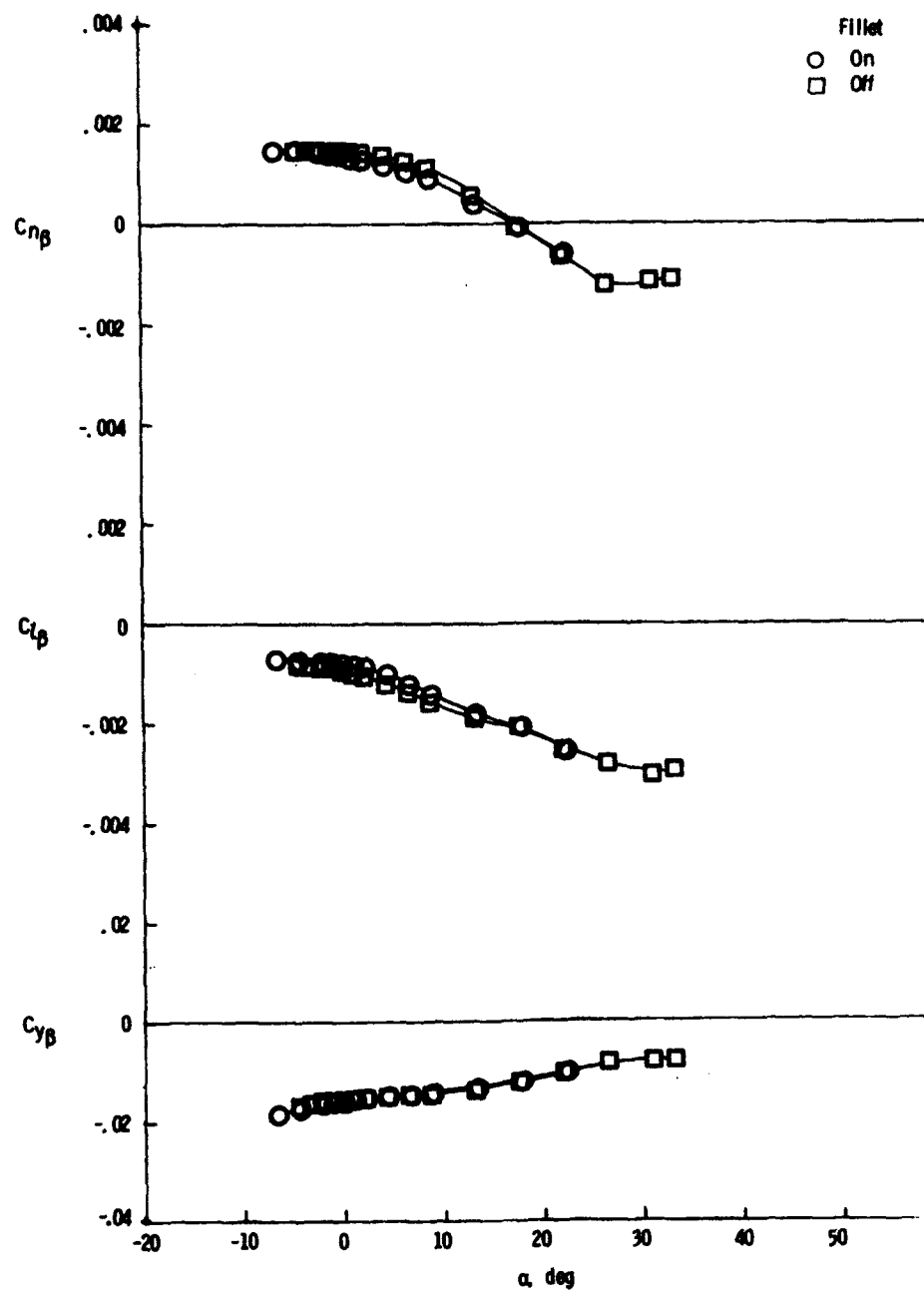
Figure 12 - Continued.



(d)  $M = 2.86$

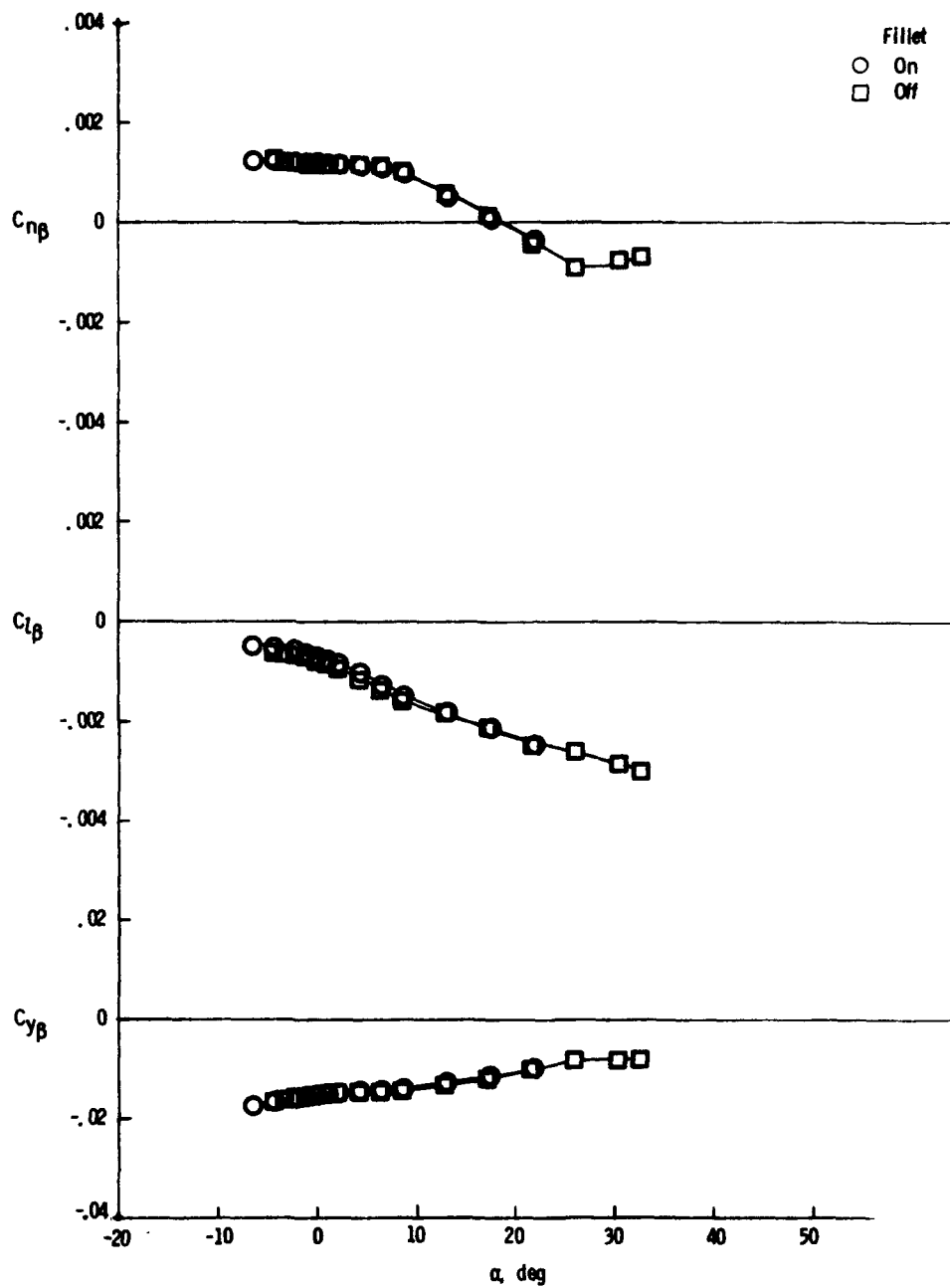
Figure 12 - Concluded.





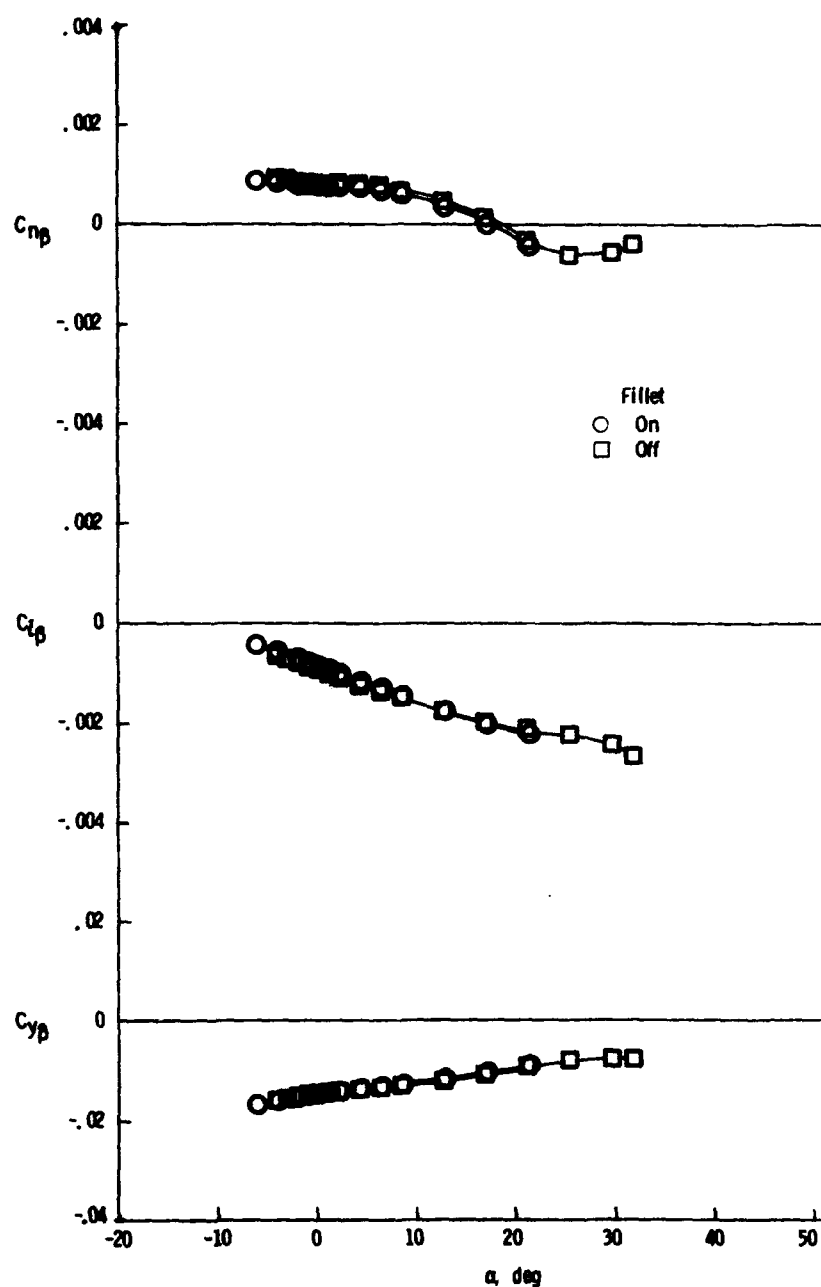
(a)  $M = 2.36$ .

Figure 13. - Effect of planform fillet on lateral-directional stability characteristics of single fin version, center fin on (flared rudder),  $\delta_e = \delta_f = 0^\circ$



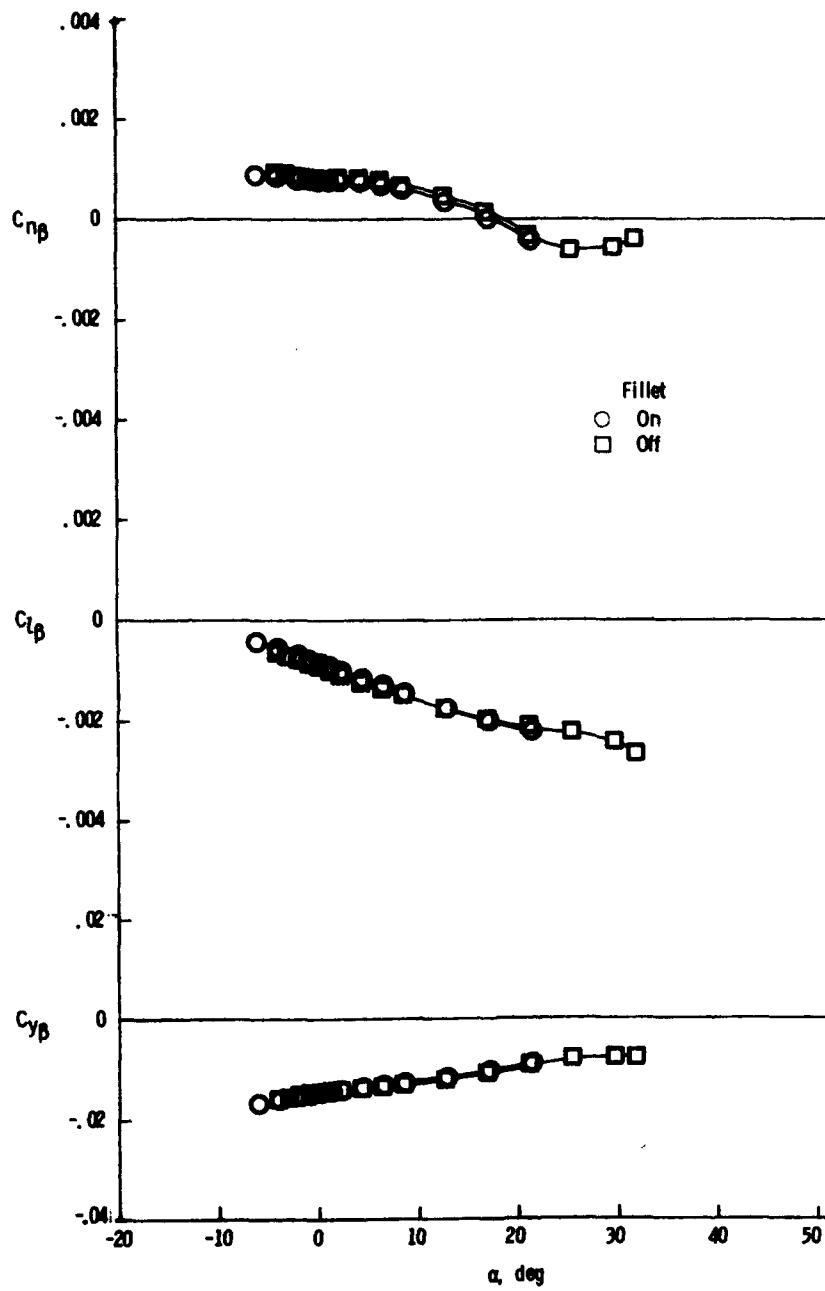
(b)  $M = 2.86$

Figure 13.- Continued.



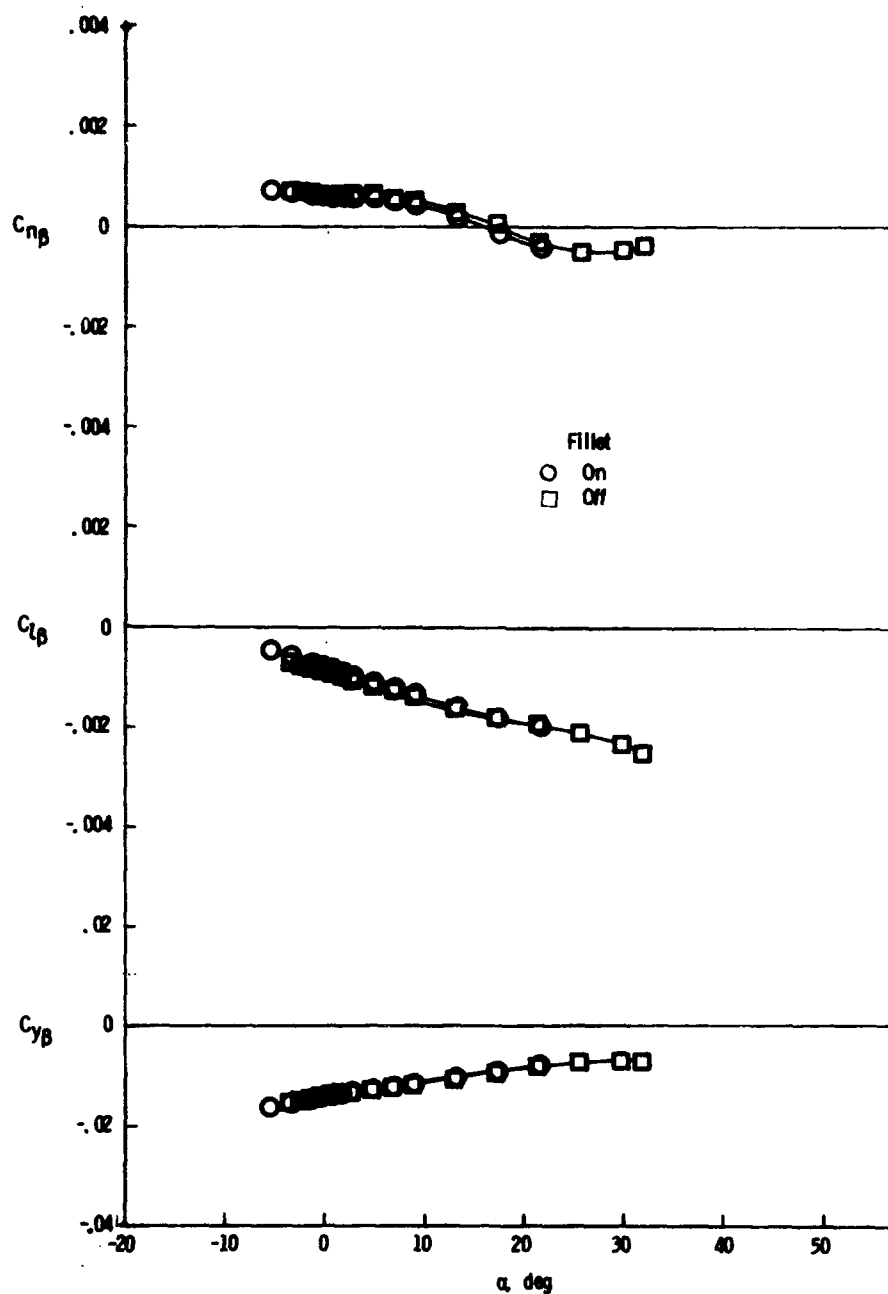
(c)  $M = 3.96$

Figure 13 - Continued.



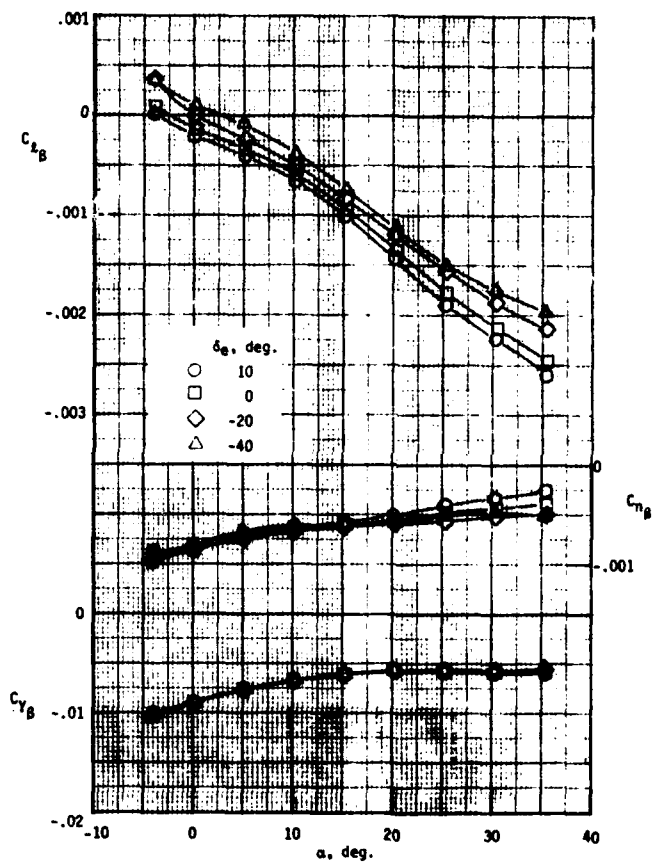
(c)  $M = 3.96$

Figure 13. - Continued.



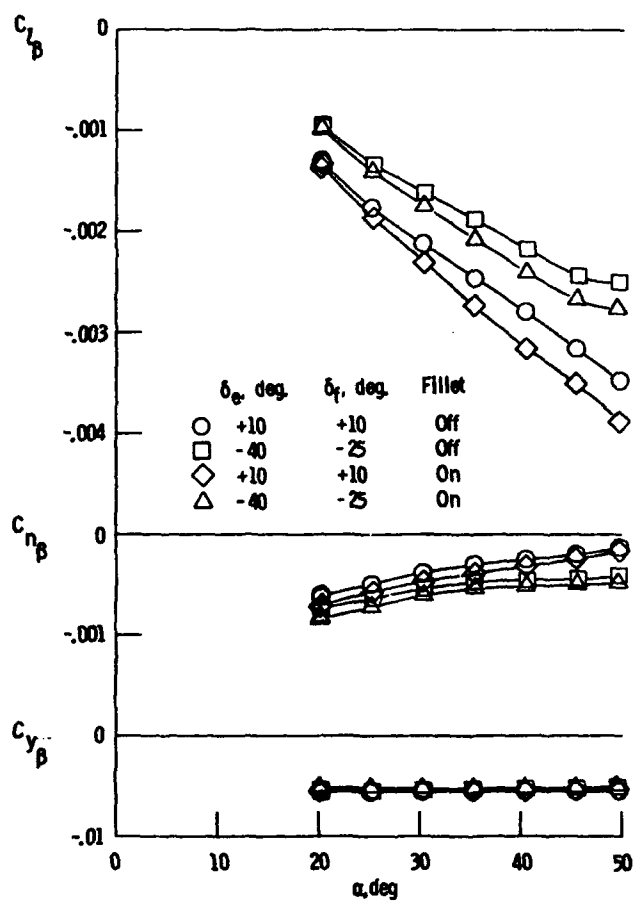
(d)  $M = 4.63$

Figure 13 - Concluded.



(a) Straight sting,  $\delta_f = 0^\circ$ , center fin on (rudder unflared).

Figure 14 - Effect of elevon and body flap deflection and planform fillet on lateral-directional stability characteristics of single fin version at  $M = 10.3$ .



(b) Bent sting, center fin off.

Figure 14. - Concluded.